AFOSR - TR - 75 - 1648

See 1473

AD A019659

FINAL REPORT

TURBULENT MIXING AND COMBUSTION

NOVEMBER 1975

F44620-70-C-0116

L. F. Moon
G. Rudinger
G. R. Salter

Textron's Bell Aerospace

DDC
RECEIVED
JAN 23 1976
A

Approved for public release; distribution unlimited.

FOR

AIR FORCE OFFICE OF SCIENTIFIC RESEARCH/NA
1400 WILSON BOULEVARD
ARLINGTON, VIRGINIA 22209

HIGH SPEED TURBULENT MIXING AND COMBUSTION

August 1970 - July 1975

SUMMARY

This program encompasses investigation of turbulent mixing and combustion processes required for advanced propulsion systems. Theoretical and experimental studies of homogeneous and heterogeneous turbulent mixing processes have been investigated. These studies resulted in the following: An eddy viscosity model was developed for axisymmetric turbulent jets. This model was demonstrated to be applicable in the core, transition and similarity regions for data covering a broad range of flow conditions. A detailed survey was made of axisymmetric jet mixing data reported in the open literature. The extension of universal jet width growth and universal decay laws to variable density flows was demonstrated to be inadequate for characterization of this class of flow. The recirculation, which occurrs in the separation region behind sudden expansions typical of modern combustors was investigated using a laser-Doppler velocimeter. Detailed measurements of the mean, axial and radial velocities were made, as well as some measurements of turbulence intensity and shear stress. A set of partial differential equations were derived and simultaneously solved. Predictions made using these equations were brought into good agreement with data taken from the recirculating flows by computer optimization of appropriate "constants" in the models.

This investigation also contributes to the understanding needed for effective utilization of powdered fuels by investigating different aspects of the problem. These studies: established feasibility of shock-tube techniques for measuring ignition delay of boron particles; found that slip of small particles to reduce diffusion limitations yields only small reductions in burning time; analyzed the effect of cross flow on penetration of injected particles; analyzed simultaneous heat, mass, and momentum addition from fuel jets injected in the upstream direction to provide more residence time for fuel particles; determined penetration correlations for light and heavy gases and gas-particle mixtures injected into a cross flow; assessed interaction of two gas-particle jets; and contributed to reviews of wave propagation and general flow properties in gas-particle mixtures.

BIBLIOGRAPHY

(1) Morgenthaler, J. H., Zelazny, S. W., and Herendeen, D. L., "Combustor Correlation Technique," Bell Report Number 9500-920208, September 1971.

(2) Morgenthaler, J H., Zelazny, S. W., and Rudinger, G., "Progress Report - High Speed Turbulent Mixing and Combustion Application to Advanced Air Breathing Propulsion Engines," Bell Report Number 9500-920212, November 1971.

(3) Zelazny, S. W., "Eddy Viscosity in Quiescent and Coflowing Axisymmetric Jets," AIAA Journal, Vol. 9, November 1971, pp. 2292-2294.

(4) Baker, A. J., Moon, L. F., Morgenthaler, J. H., and Peschke, W. T., "Fluid Mechanics and Combustion Technology," Bell Report Number 9500-920246, January 1972.

(5) Morgenthaler, J. H. and Zelazny, S. W., "Predictions of Axisymmetric Free Turbulent Shear Flows Using a Generalized Eddy Viscosity Approach," Proceedings of the NASA Workshop on Free Turbulent Shear Flows, Conference Proceedings, Vol. I, NASA SP-321, July 1972.

(6) Zelazny, S. W., "Modeling of Turbulent Axisymmetric Coflowing Streams and Quiescent Jets: A Review and Extension," PhD Dissertation, State University of New York at Buffalo, September 1972.

(7) Morgenthaler, J. H., Zelazny, S. W., and Rudinger, G., "Progress Report - High Speed Turbulent Mixing and Combustion," Bell Report Number 9500-920258, December 1972.

(8) Rudinger, G., "Wave Propagation in Suspensions of Solid Particles in Gas Flow," Applied Mechanics Reviews, Vol. 26, March 1973, pp. 273-279.

(9) Zelazny, S. W., Morgenthaler, J. H., and Herendeen, D. L., "Shear Stress and Turbulence Intensity Models for Coflowing Axisymmetric Streams," AIAA Journal, Vol. 11, August 1973, pp. 1165-1173.

(10) Morgenthaler, J. H. and Rudinger, G., "Progress Report - High Speed Turbulent Mixing and Combustion," Bell Report Number 9500-920316, November 1973.

(11) Zelazny, S. W., "Study of Methods for Modeling Centerline Mass Fraction Decay in Turbulent Jets," AIAA Journal, Vol. 12, No. 2, February 1974, pp. 235-237.

(12) Rudinger, G., "Experimental Investigation of Gas Injection Through a Transverse Slot into a Subsonic Cross Flow," AIAA Journal, Vol. 12, April 1974, pp. 566-568.

(13) Morgenthaler, J. H., "Turbulent Mixing and Reacting Flow Characterization," Fluid Mechanics of Combustion, ASME, New York, May 1974, pp. 21-34.

(14) Rudinger, G., "Effects of Velocity Slip on the Burning Rate of Fuel Particles," Fluid Mechanics of Combustion, ASME, New York May 1974, pp. 35-46.

(15) Rudinger, G., "Simultaneous Heat, Mass, and Momentum Addition to a Gas Flow in a Pipe," ASME Paper No. 74-FE-14, May 1974.

(16) Rudinger, G., "Penetration of Particles Injected into a Constant Cross Flow," AIAA Journal, Vol. 12, No. 8, August 1974, pp. 1138-1140.

(17) Morgenthaler, J. H., Moon, L. F., and Stepien, W. R., "Developing a Gas Rocket Performance Prediction Technique," NASA CR-134728, October 1974.

(18) Rudinger, G., "Progress Report - High Speed Turbulent Mixing and Combustion," Bell Report Number 9500-920351, November 1974.

(19) Moon, L. F. and Zelazny, S. W., "Experimental and Analytical Study of Jet Noise Modeling," AIAA Journal, Vol. 13, No. 3, March 1975, pp. 387-393.

(20) Rudinger, G., "Effect of Velocity Slip on the Burning Rate of Fuel Particles," Journal of Fluids Engineering, Trans. ASME, Vol. 97I, No. 3, September 1975, pp. 321-326.

(21) Moon, L. F., Rudinger, G., and Salter, G. R., "Final Report - High Speed Turbulent Mixing and Combustion," Bell Report Number 9500-920350, November 1975.

(22) Morgenthaler, J. H., "Turbulent Mixing and Reacting Flow Characterization," scheduled for publication in the Journal of Fluids Engineering, Trans. ASME, December 1975.

(23) Rudinger, G., "Fundamentals and Applications of Gas-Particle Flow," to be published in a forthcoming AGARDograph.

(24) Rudinger, G., "Some Aspects of Gas-Particle Jets in a Cross Flow," submitted for publication in the ASME Journal.

(25) Moon, L. F., Rudinger, G., and Salter, G. R., "Velocity Distribution in an Abruptly Expanding Circular Duct," submitted for publication in the ASME Journal.

ABSTRACT

The behavior of recirculating flows typical of advanced air-breathing and rocket injectors, as well as high energy chemical lasers, have been experimentally investigated. The configuration used consisted of a circular duct having a sudden increase of its diameter. Step size and flow velocity were chosen to be of a magnitude representative of "sudden-dump" combustion chambers. The recirculation, which occurred in the separation region behind the sudden expansion, was investigated using a laser-Doppler velocimeter. Detailed measurements of the mean, axial, and radial velocities were made, as well as some measurements of turbulence intensity and shear stress. A set of partial differential equations - including continuity, axial and transverse momentum, turbulence energy, and turbulence dissipation - were derived and simultaneously solved using both integral and finite differencing techniques. Predictions made using these equations were brought into good agreement with the data taken from the recirculating flows under investigation by computer optimization of appropriate "constants" in the models.

F44620-70-C-0116

AIR FORCE OFFICE OF SCIENTIFIC RESEARCH (AFSC)
NOTICE OF TRANSMITTAL TO DDC
This technical report has been reviewed and is approved for public release IAW AFR 190-12 (7b).
Distribution is unlimited.
A. D. BLOSE
Technical Information Officer

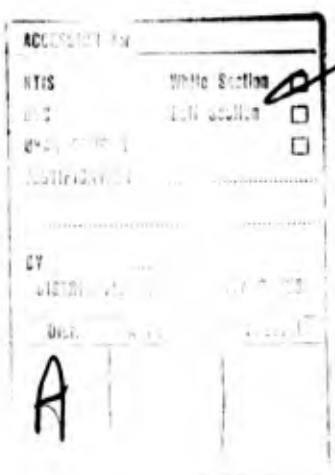

CONTENTS

NOMENCLATURE

b	Boundary layer width
B	Step height
D	Internal diameter of larger tube
f	Doppler frequency
G	See Equation (51)
h	Radial distance from centerline to surface separating the forward and back flows
k	Turbulence kinetic energy
ℓ_1	Axial distance from step to vortex center
ℓ_2	Axial distance from vortex center to reattachment point
m	Velocity ratio
P	Probability or pressure
R	Internal radius of larger tube
u	Local velocity
U	Time averaged velocity
V	Velocity
x	Axial distance from step
y	Distance from the wall
α	Angle between velocity vector and axis of duct (see Figure 3)
η	Similarity parameter
θ	Angle between beams of laser-Doppler system (see Figure 2
λ	Wavelength of laser light
σ	Standard deviation

ϕ	Angle between optical axis of laser-Doppler system and normal to the axis of duct
ρ	Density
μ	Viscosity
μ_{eff}	Effective viscosity
μ_t	See Equation (50)
ϵ	Turbulence dissipation

Subscripts and Superscripts

a	Axial direction
b	"Blue" laser-Doppler system
g	"Green" laser-Doppler system
i	Tensor index
j	Tensor index
n	Two-dimensional parameters used in potential flow analysis
r	Radial direction
$'$	Prime, denotes fluctuations
$\bar{}$	Bar, mean value

ILLUSTRATIONS

I. SUMMARY

Calculation of turbulent flow fields involves modeling of the turbulence properties in the form of turbulent kinetic energy, an eddy viscosity, or some other model[1,2]. Such models are derived on the basis of a hypothesis, such as Prandtl's "mixing length," but ultimately, experimental data for mean velocity and turbulence parameters are needed to develop or test a model. Many experimental studies are available for flows of the boundary-layer type in which the mean flow has a predominant direction, but a great need still exists for experimental data on more complicated flows, particularly, flows with recirculation regions. Recirculation occurs in the separation region behind sudden, or sufficiently rapid, expansion of the flow. Such flows are utilized, for example, for flame holding and mixing in combustion chambers or chemical lasers[3,4,5].

Aim of the present experimental study is to contribute to the knowledge about recirculating flows. The configuration used consists of a circular duct having a sudden increase of its diameter. Step size and flow velocity were chosen to be of a magnitude representative of "sudden-dump" combustion chambers.

Experimental observations were made in a transparent test section. Initially, an estimate of the extent of the recirculation zone was obtained by a simple flow visualization technique. Measurements of mean velocity and of some turbulence fluctuations were made with a laser-Doppler velocimeter along several traverses across the duct in the region of interest. It should be noted that the flow reversals which occur in the recirculation zone and the large turbulence fluctuations in a region of near-zero velocity preclude the use of hot-wire techniques. Even the laser Doppler method requires a frequency shift in one beam to provide an unambiguous relationship between velocity and Doppler frequency shift.

These experiments located both the dividing streamline which separates the main flow from the recirculation region and the location of flow reversal within the recirculation region. Two analytical models for these features also were developed.

The experimental setup and results are discussed in the following sections.

II. EXPERIMENTAL SETUP

A schematic drawing of the test section is shown in Fig. 1. Two lucite tubes with a connecting plug form a duct in which the inside diameter suddenly increases from 2.75 in. (70 mm) to 4.00 in. (102 mm). This plug is cemented to the smaller tube and can slide inside the larger one. Thus, the test region behind the step can be kept within the length covered by the optical windows described below. The narrow tube is about 18 diameters long and is provided with a flaired inlet. The larger tube has about the same length-to-diameter ratio and is connected by a flexible hose to a vacuum pump. The flow can be adjusted by a variable by-pass. A pitot-static tube is mounted at the center of the smaller tube and is used for adjustment of the flow to the desired velocity. The laser-Doppler system requires fine particles in the flow which are injected into the small tube some distance upstream from the step. Equally good results were obtained by injecting the particles into the air near the inlet to the smaller tube. The entire tube assembly is supported by a 4 in. aluminum channel which is mounted on the bed of a milling machine. This arrangement allows the entire test section to be precisely moved in three dimensions relative to the optical system which is mounted on a rigid table.

The particles required for the laser-Doppler measurements are produced by a conventional LaMer-Sinclair generator as described by Liu, Whitby and Yu[6]. It produces a spray of dibutyl-phtalate droplets having diameters of a fraction of one micrometre. A slot of about 10 mm width and 130 mm length is cut in opposite sides of the test section to allow mounting of optically flat windows for the laser-Doppler system (see inset of Fig. 1). For this slot width, the cylindrical wall shape of the duct is practically undisturbed.

III. LASER-DOPPLER TECHNIQUE

The well-known principle of the laser-Doppler technique[7] is shown in Fig. 2. A primary laser beam is split into two beams by the beam splitter S. These beams are focused on the test point T by means of the two mirrors M_1 and M_2 and lens L_1. At T, the component V of the flow velocity at right angles to the axis of the optical system and in the plane of the two laser beams produces a Doppler frequency shift f in the light scattered from a tracer particle at the test point. The velocity of this particle then is related to the wavelength of the laser light λ and the geometry of the system by

$$V = \frac{\lambda f}{2\sin(\theta/2)} \qquad (1)$$

where θ, the angle between the focused beams, was 9.7° in all experiments. The scattered light can be picked up in any direction, but its intensity is particularly strong near the axis of the system. It is focused by the lens L_2 on the pin hole H, which reduces extraneous light and is finally received by a photomultiplier.

Because of the finite dimensions of the laser beams, the test point T represents a finite volume which however is much smaller than 1 mm^3. As tracer particles pass through this volume, they produce Doppler signals which are amplified, monitored on an oscilloscope and recorded by a spectrum analyzer.

To obtain an adequate Doppler signal, the laser had to be operated at a power level of about 150 mW. In spite of anti-reflection coating of the windows and frequent cleaning from deposited oil droplets, measurements could not be made closer than about 2 mm from the wall because of excessive scattered light. The light scattered from the laser beams inside the glass could be seen through laser safety goggles. With the help of a magnifier, it was thus possible to locate the intersection

of the two laser beams on the wall with an accuracy of at least 0.1 mm. Traverses across the duct always were measured from the wall.

The flow velocity reverses in a recirculation zone and also in a turbulent flow with near-zero mean velocity. In such regions, Eq. (1) would yield erroneous results, because the Doppler frequency shift does not depend on the flow direction. This problem is overcome by shifting the frequency of one of the laser beams by a constant amount. The shift is accomplished[7] by inserting a Bragg cell B, driven by a high-frequency oscillator, as shown in Fig. 2. The Doppler frequency shift in Eq. (1) then must be interpreted as $f-f_s$, where f_s is the frequency shift produced by the Bragg cell. All experiments were performed with f_s = 40 MHz. Thus, Doppler frequencies greater than 40 MHz indicate a positive velocity, while frequencies below 40 MHz indicate a negative velocity.

The major components used for these experiments are:

Laser: Spectra Physics Argon Laser, Type 165
Amplifier: Hewlett-Packard, Type HF8447A
Photomultiplier: RCA, Type 8645
Bragg Cell: Zenith Light Modulator, Type M-40
Spectrum Analyzer: Hewlett-Packard, Type 141T-85528-8553B

The injected particles are small enough to follow turbulent velocity fluctuations. After a sampling time of several seconds, the screen of the spectrum analyzer shows the velocity (frequency) distribution of the particles which have passed through the test volume. Their mean velocity $\bar{V}$ can be read from the screen image with an accuracy of about 0.5 MHz by carefully estimating the frequency which divides the distribution into two equal areas.

Turbulent fluctuations V' are indicated by the spread of the distribution curve. Let the velocity of a particle that passes through the test volume be given by $V = \bar{V}+V'$, and let the

probability that a fluctuation lies between V′ and V′+dV′ be given by P(V′)dV′. This probability is related to the standard deviation σ of the distribution by

$$\sigma^2 = \overline{V'^2} = \int_{-\infty}^{+\infty} V'^2 P(V')dV' \qquad (2)$$

If the fluctuations followed a Gaussian distribution[8], the probability distribution would be given by

$$P(V') = \frac{1}{\sigma\sqrt{2\pi}} e^{-V'^2/2\sigma^2} \qquad (3)$$

The value of P(V′) for which V′ = σ then follows from

$$\frac{P(\sigma)}{P(0)} = e^{-0.5} = 0.606 \qquad (4)$$

Thus, the standard deviation of a Gaussian distribution can be found as the value of V′ for which the distribution curve has 60% of its maximum value. The "half-width" of the distribution, where P(V′)/P(0) = 0.5, yields a value of V′ that is only 17% larger than σ.

The distribution of V′ in a turbulent flow often is not Gaussian[8], and the half-width, determined from the spectrum analyzer, was used as a reasonable value for the root-mean square value of the turbulence fluctuations. A more refined method would have to be based on direct evaluation of the integral in Eq. (2) from photographs of the frequency spectrum, which would have been prohibitive for the many measurements required, or with the aid of automatic electronic counting and computing equipment, which was not available for the required frequency range.

One laser-Doppler system can measure only one velocity component. In the present experimental setup, it readily can sense the mean of the axial velocity $\overline{V}_a$ and its fluctuations $\overline{V'_a}$. Because of the cylindrical walls and the narrow width of the windows, it is not possible to measure radial velocities

directly. An attempt was made to measure the radial velocities $\overline{V}_r$ and $\overline{V'_r}$ and the covariance $\overline{V'_r V'_a}$ by using simultaneously two laser-Doppler systems as indicated in Fig. 1. Two different wavelengths were used to distinguish between the scattered light from each system: a green line with λ = 514.5 nm and a blue line with λ = 488 nm. Interference filters were used to prevent the light from one system to reach the photomultiplier of the other.

For the elements used in these systems, velocities were obtained from

$$V_g = 3.04\ f \text{ for the "green" system}$$
$$V_b = 2.89\ f \text{ for the "blue" system} \qquad (5)$$

These equations yield the velocity in m/s if the appropriate Doppler frequency is given in MHz.

Since the optical axes of the two laser systems are not at right angles to the axis of the flow, the "green" and "blue" velocities V_g and V_b are of no direct interest. The axial and radial velocity components V_a and V_r must be determined from V_g and V_b by considering the geometric relationships as indicated in Fig. 3. Assume that the flow velocity V forms the angle α with the axis of the flow, and let the angles between the axis of the green and blue beams with the normal to the flow axis be denoted by ϕ_g and ϕ_b. The velocity components measured by the laser-Doppler systems, V_g and V_b, also form the angles ϕ_g and ϕ_b with the flow axis, and the following relationships are evident

$$V_g = V\cos(\phi_g - \alpha) = V(\cos\phi_g\cos\alpha + \sin\phi_g\sin\alpha)$$
$$V_b = V\cos(\phi_b + \alpha) = V(\cos\phi_g\cos\alpha - \sin\phi_g\sin\alpha) \qquad (6)$$

If $V_a = V\cos\alpha$ and $V_r = V\sin\alpha$ are substituted into Eqs. (6), one obtains two equations for the unknown V_a and V_r with the solution

$$V_a = \frac{V_g \sin\phi_b + V_b \sin\phi_g}{\sin(\phi_g + \phi_b)}$$

$$V_r = \frac{V_g \cos\phi_b - V_b \cos\phi_g}{\sin(\phi_g + \phi_b)} \qquad (7)$$

In the present setup, the angles ϕ_g and ϕ_b were equal and $\phi_g = \phi_b = \phi = 15.74^o$. Then, Eqs. (7) simplify to

$$V_a = \frac{V_g + V_b}{2\cos\phi}$$

$$V_r = \frac{V_g - V_b}{2\sin\phi} \qquad (8)$$

where V_g and V_b must be obtained from Eqs. (5).

Equations (5) and (6) apply both to the instantaneous velocities and to their mean values. Thus, $\overline{V}_a$ and $\overline{V}_r$ are directly obtainable, but the fluctuations require further analysis because only $V_g'^2$ and $V_b'^2$ are directly measured by the spectrum analyzer. From the definition of the quantities involved, it follows that

$$V_a + V_a' = \frac{1}{2\cos\phi} (\overline{V}_g + V_g' + \overline{V}_b + V_b')$$

or

$$V_a' = \frac{1}{2\cos\phi} (V_g' + V_b') \qquad (9)$$

and similarly

$$V_r' = \frac{1}{2\sin\phi} (V_g' - V_b') \qquad (10)$$

If Eqs. (9) and (10) are squared and a time average is taken over a sufficiently long time, all linear terms become equal to zero, and one obtains

$$\overline{v_a'^2} = \frac{1}{4\cos^2\phi}\left(\overline{v_g'^2} + \overline{v_b'^2} + 2\,\overline{v_g'v_b'}\right)$$

$$\overline{v_r'^2} = \frac{1}{4\sin^2\phi}\left(\overline{v_g'^2} + \overline{v_b'^2} - 2\,\overline{v_g'v_b'}\right) \qquad (11)$$

Clearly, Eqs. (11) are not yet sufficient to compute the fluctuation quantities $\overline{v_a'^2}$ and $\overline{v_r'^2}$ since the covariance $\overline{v_g'v_b'}$ is not known. This problem was solved by exploring the flow field not only with the two-color system as described but also with a one-color system with its optical axis aligned at right angles to the flow axis to measure $\overline{v_a'}$ and $\overline{v_a'^2}$ directly. If the value of $\overline{v_a'^2}$ is substituted into the first of Eqs. (11), the equation can be solved for $\overline{v_g'v_b'}$ which together with the second equation yields $\overline{v_r'^2}$ in the form

$$\overline{v_r'^2} = \frac{1}{4\sin^2\phi}\left(\overline{v_g'^2} + \overline{v_b'^2} - 2\cos^2\phi\;\overline{v_\varepsilon'^2}\right) \qquad (12)$$

The covariance $\overline{v_a'v_r'}$ is obtained in a similar manner from

$$(V_a+v_a')(V_r+v_r') = \frac{1}{4\sin\phi\cos\phi}(V_g+v_g'+V_b+v_b')(V_g+v_g'-V_b-v_b')$$

After subtracting the equation for the mean values alone

$$V_a V_r = \frac{1}{4\sin\phi\cos\phi}\left(V_g^2 - V_b^2\right)$$

and time averaging the remaining terms, one finally obtains

$$\overline{v_a'v_r'} = \frac{1}{2\sin^2\phi}\left(\overline{v_g'^2} - \overline{v_b'^2}\right) \qquad (13)$$

The spectrum on the screen of the frequency analyzer is not well defined, and the accuracy of the measured fluctuations thus is not high. Therefore, only rough qualitative results should be expected for $\overline{v_r'^2}$ and $\overline{v_a'v_r'}$, since calculation of these terms involves the difference between other fluctuation terms.

According to the foregoing, the axial mean velocity $\bar{V}_a$ was measured both with the one-color and the two-color system. Comparison of the results thus provided a check of the measurements and increased confidence in the data. The majority of the measurements were performed with the one-color system.

IV. EXPERIMENTAL RESULTS

A number of traverses across the test section are needed to explore the flow field in the recirculation region. Since the extent of the latter was not known beforehand and the available funds allowed only a few traverses to be made, preliminary experiments were performed to establish the approximate extent of the region of interest. A fine jet of particles - the same as those used subsequently for the laser-Doppler experiments - was directed from a capillary tube against the inside wall of the test section. The tip of the capillary tube was about one-half of the step height away from the wall. The jet was illuminated through the wall of the test section by a small He-Ne laser. As it was moved through the recirculation zone, one could observe if it was deflected in the upstream or in the downstream direction. These experiments indicated that the location of flow reversal is practically independent of the flow velocity over the range from about 40 to 90 m/s in the smaller tube. The region of interest extended from the step to about 1.5 duct diameters downstream. These data, in addition to data taken from Refs. 9, 10, and 11, are included in Fig. 4. This figure shows the variation of reattachment length with Reynolds number for flows in suddenly expanding circular ducts. Results from this investigation are for higher Reynolds numbers than have previously been reported; however, these results, as well as those reported in Refs. 9, 10, and 11, all show the reattachment length for turbulent flows to be between six and nine step heights.

The laser-Doppler systems were set up and several traverses made between the axis of the duct and the wall at different distances x from the step of the test section. The center velocity in the smaller tube at the entrance to the larger one was 64.8 m/s (210 ft/s) for all experiments. This velocity corresponds to a Reynolds number based on the small tube diameter of about 2.8×10^5 and assures fully developed turbulent pipe flow in the

smaller tube. As described in the preceding section, both the one-color and the two-color systems were used for the measurements.

The mean axial velocity $\bar{V}_a$ at x/D = 0.75 (D is the internal diameter of the larger tube) is shown in Fig. 5 as a function of the nondimensional distance from the wall, y/D, as obtained by both LDV systems. The rather good agreement between these data strengthens the confidence in the results. For this traverse, the point where the axial flow reverses ($\bar{V}_a = 0$) is located at y/D = 0.09.

Results for the mean axial velocity at several distances from the step are collected in Fig. 6. These were obtained with the one-color system. It can be seen that there is no flow reversal for x/D greater than about 1.25. It also may be noted that the velocity in the center of the tube decreases only slowly with increasing distance from the step. The flow from the smaller tube into the larger one thus acts at first as if it were a free jet. At x/D = 3, the center velocity has fallen to 38 m/s, and the velocity distribution approaches the shape of a fully developed turbulent flow. The total flow rate through the duct was determined by integration of one of the profiles, and the corresponding profile of the fully developed turbulent flow was computed[12]. It is entered in Fig. 6 as the broken line. The gradual decrease of the center velocity is shown also in Fig. 7 from which one may estimate that a fully developed turbulent flow is re-established at a distance of about four duct diameters from the step.

The points where the axial flow velocity reverses ($\bar{V}_a = 0$) can be found directly from Fig. 6, and the locus of these points is indicated in Fig. 8 by the triangles. It is of interest also to find the dividing streamline which separates the recirculation zone from the main flow. It can be found by considering that there is no net flow through the region between the wall and the dividing streamline. The net flow between the wall and a circle

of radius R-y is given by $2\pi\int_0^y \bar{V}_a(R-y')dy'$, where R is the radius of the tube. This integration was performed numerically for all traverses made within the recirculation zone, and the value of y was determined for which the integral vanished. The resultant points of the dividing streamline are indicated in Fig. 8 by circles.

The stagnation point, where the dividing streamline reaches the wall of the tube, could not be determined in this manner, because measurements could not be made sufficiently close to the wall (see preceding section). However, it could be found by the following simple experiment: A small amount of water was poured into the duct. It was dispersed by the flow into small droplets which were deposited on the wall and driven by the flow in either the upstream or downstream direction. The stagnation point, where they remained at rest, could be located to within a few millimeters. This point, x/D ~ 1.3, also is shown in Fig. 8 and is consistent with the other experimental data. The dividing streamline at first runs nearly parallel to the wall and approaches it only in the vicinity of the stagnation point. The shape of this curve appears exaggerated in Fig. 8 because of the different scales used for the abscissa and ordinate.

Axial turbulence intensities at four distances from the step are shown in Fig. 9. These were obtained directly with the one-color system and are expressed in terms of a constant reference velocity, selected as V_{ref} = 64.8 ms - the center velocity at the entrance to the larger tube. The turbulence level near the center of the tube is a little over 10%. It increases sharply to a maximum over 40% which, for all traverses, is located near y/D = 0.13. This distance corresponds approximately to the step height (see Fig. 8). As the wall is approached further, the intensity decreases again. Qualitatively, this is the behavior that one should expect in the recirculation region. The fact that the same behavior is observed also downstream of this region

indicates a slow decay of the high turbulence levels. Correspondingly, the maxima of the curves in Fig. 9 also decrease with increasing values of y/D. The decrease of the intensity to zero at the wall must be quite precipitous, because the intensity is still between 20 and 30% at y/D = 0.025 (about 2.5 mm). The local turbulence intensity, that is, $\overline{V_a'^2}$ divided by the local value of $\bar{V}_a$ is much higher than the values given by Fig. 9 because of the decrease of $\bar{V}_a$ as the wall is approached. It is in the neighborhood of 80% in the region of the turbulence maxima in Fig. 8 and goes well above 100% closer to the wall.

As discussed in the preceding section, the covariance, $\overline{V_a'V_r'}$, is obtained by using the two-color LDV system, while the radial intensity, $\overline{V_r'^2}$, requires the additional use of the one-color system. Furthermore, these quantities involve differences of experimental data which themselves cannot be measured with great accuracy. The numerical results obtained for $\overline{V_r'^2}$ scattered too much to be of direct value but indicate the expected behavior; they are small near the axis of symmetry, have a maximum at or near the location of the maximum of $\overline{V_a'^2}$ of comparable magnitude and decrease again as the wall is approached.

The covariance is proportional to the Reynolds shear stress ($\tau = -\rho\,\overline{V_r'V_a'}$, where ρ is the gas density) and is negative in a turbulent pipe flow. The best measured data are shown in Fig. 10, where the dimensionless values $\overline{V_a'V_r'}/V_{ref}^2$ are plotted against distance from the step. As required, the covariance is zero at the center of the flow. It reaches negative values as in a pipe flow but, after reaching a minimum, increases again and becomes positive near the wall as necessary for recirculating flow.

V. THEORY

V.1 Integral Approach

Figure 11 shows a cross-sectional view of the duct in the region of the sudden expansion. The radius of the larger duct is R and the step height is B. A rectangular Cartesian coordinate system is selected such that the origin, 0, is located at the edge of the step, with the x-axis parallel to the duct centerline and the y-axis pointing inward through the duct axis. The center of the vortex, which is denoted by the numeral 4 in Fig. 11, is located in the plane MM′ at a distance $x = \ell_1$. The locus of the inner surface of the boundary layer is 011′ and the outer surface is 02. The locus of zero axial velocity is the surface 04N, and the dividing stream surface between the returning flow, and the continuing flow is 03N. N is the reattachment ring, at a distance ℓ_2 from the plane MM′. ZZ′ is any intermediate plane between the step plane KK′ and the plane MM′. The undisturbed duct velocity, which is assumed to have a flat profile, is denoted by u_1; the back flow velocity in the annulus between the boundary layer outer surface and the duct wall is u_2, and the velocity in the boundary layer is u. The duct wall boundary layer is not included in the analysis.

Following Abramovich's analysis of turbulent two-dimensional step flow and axisymmetric flow over bluff bodies[13], the pressure across any plane ZZ′ is assumed to be constant, and the momentum balance for the zone KK′Z′Z may be written as

$$u_1^2(R-B)^2 = u_1^2(R-B-y_1)^2 + 2\int_{y_2}^{y_1} u^2(R-B-y)dy + u_2^2[R^2-(R-B-y_2)^2] \quad (14)$$

Assuming the following form for the boundary layer velocity profile

$$\frac{u_1 - u}{u_1 - u_2} = f(\eta) = (1-\eta^{1.5})^2$$

where $\eta = \frac{y - y_2}{b}$, b being the boundary layer width $(y_1 - y_2)$, and writing $\bar{b} = b/B$, $R' = R/B$ and $R'' = (R-B)/B$, Eq. (14) becomes

$$\left(\frac{y_1}{B}\right)^2 - 2R''\left(\frac{y_1}{B}\right) + 2\bar{b}\int_0^1 \left[1-(1-m)(1-\eta^{1.5})^2\right]^2 (R'' - \frac{y_2}{B} - \eta\bar{b})d\eta + m^2(1 + \frac{y_2}{B})(R'+RR'' - \frac{y_2}{B}) = 0 \qquad (15)$$

where $m = u_2/u_1$.

After integration, Eq. (15) is

$$\left(\frac{y_1}{B}\right)^2 - 2R''\left(\frac{y_1}{B}\right) + \bar{b}(R'' - \frac{y_2}{B})\left[2-1.8(1-m) + 0.6312(1-m)^2\right] - (\bar{b})^2\left[1-0.5142(1-m) + 0.1336(1-m)^2\right] + (1 + \frac{y_2}{B})(R'+R'' - \frac{y_2}{B})m^2 = 0 \qquad (16)$$

The continuity equation for zone KK'Z'Z may be expressed as

$$u_1(R-B)^2 = u_1(R-B-y_1)^2 + 2\int_{y_2}^{y_1} u(R-B-y)dy + u_2\left[R^2-(R-B-y_2)^2\right] \qquad (17)$$

Transformed to dimensionless coordinates, Eq. (17) becomes

$$\left(\frac{y_1}{B}\right)^2 - 2R'' \left(\frac{y_1}{B}\right) + 2\bar{b}\int_0^1 \left[1-(1-m)(1-\eta^{1.5})^2\right](R'' - \frac{y_2}{B} - \eta\bar{b})d\eta + m(1 + \frac{y_2}{B})(R'+RR'' - \frac{y_2}{B}) = 0 \qquad (18)$$

Carrying out the integration, the resulting continuity equation becomes

$$\left(\frac{y_1}{B}\right)^2 - 2R'' \left(\frac{y_1}{B}\right) + \bar{b}(R'' - \frac{y_2}{B})(1.10+0.90m) - (\bar{b})^2(0.7428+0.2572m) + (1 + \frac{y_2}{B})(R +R'' - \frac{y_2}{B})m = 0 \qquad (19)$$

For continuity within the circulation zone, we have

$$2\int_{y_2}^{y_3} u(R-B-y)dy + u_2\left[R^2-(R-B-y_2)^2\right] = 0 \qquad (20)$$

which can be written in the non-dimensional form as

$$2\bar{b}\int_0^{\eta_3}\left[1-(1-m)(1-\eta^{1.5})^2\right](R'' - \frac{y_2}{B} - \eta\bar{b})d\eta$$
$$+ (1 + \frac{y_2}{B})(R'+R'' - \frac{y_2}{B})m = 0 \qquad (21)$$

After integration, Eq. (21) becomes

$$2\bar{b}(R'' - \frac{y_2}{B})\left[\eta_3-(\eta_3-0.80\eta_3^{2.5}+0.25\eta_3^4)(1-m)\right]$$
$$- (\bar{b})^2\left[\eta_3^2-(\eta_3^2-1.14\eta_3^{3.5}+0.40\eta_3^5)(1-m)\right]$$
$$+ (1 + \frac{y_2}{B})(R'+RR'' - \frac{y_2}{B})m = 0 \qquad (22)$$

where $\eta_3 = (\frac{y_3}{B} - \frac{y_2}{B})\bar{b}$.

The ordinate of the zero axial velocity surface may be determined from the condition

$$u = 1-(1-m)(1-\eta_4^{1.5})^2 = 0$$

with

$$\eta_4 = (\frac{y_4}{B} - \frac{y_2}{B})/\bar{b}$$

Solving for y_4/B, yields

$$\frac{y_4}{B} = \frac{y_2}{B} + \bar{b}\left[1-(1-m)^{-1/2}\right]^{2/3} \tag{23}$$

If we assume that the increase in boundary layer thickness is the same as for a free jet then

$$b = 0.22x \tag{24}$$

Equations (16), (19), (22), (23), and (24) are sufficient for the determination of y_1, y_2, y_3, y_4, and u_2 as functions of R, B, x, and u_1 in the region KK´M´M.

Making the assumption that the energy of the forward flow is equal to the energy of the back flow in the circulation zone at the plane MM´, leads to the equation

$$\int_{y_4}^{y_3} u^3(R-B-y)dy + \int_{y_2}^{y_4} u^3(R-B-y)dy + \frac{u_2^3}{2}\left[R^2-(R-B-y_2)^2\right] = 0 \tag{25}$$

Combining the integrals and transforming to dimensionless form gives

$$2\bar{b}\int_0^{\eta_3}\left[1-(1-m)(1-\eta^{1.5})^2\right]^3(R'' - \frac{y_2}{B} - \eta\bar{b})d\eta$$

$$+ m^3(1 + \frac{y_2}{B})(R'+RR'' - \frac{y_2}{B}) = 0 \tag{26}$$

Solving the integral results in the equation

$$2\bar{b}(R'' - \frac{y_2}{B})\Big[\eta_3 - 3(1-m)(\eta_3 - \frac{\eta_3^{2.5}}{2.5}) + 3(1-m)^2(\eta_3 - 2\frac{\eta_3^{2.5}}{2.5} + \frac{\eta_3^4}{4} - (1-m)^3(\eta_3 - 3\frac{\eta_3^{2.5}}{2.5} + \frac{3\eta_3^4}{4} - \frac{\eta_3^{5.5}}{5.5})\Big] - 2(\bar{b})^2\Big[\frac{\eta_3^2}{2} - 3(1-m)(\frac{\eta_3^2}{2} - \frac{\eta_3^{3.5}}{3.5}) + 3(1-m)^2(\frac{\eta_3^2}{2} - \frac{2\eta_3^{3.5}}{3.5} + \frac{\eta_3^5}{5}) - (1-m)^3(\frac{\eta_3^2}{2} - \frac{3\eta_3^{3.5}}{3.5} + \frac{3}{5}\eta_3^5 - \frac{\eta_3^{6.5}}{6.5})\Big] + m^3(1 + \frac{y_2}{B})(R'+RR'' - \frac{y_2}{B}) = 0 \qquad (27)$$

The x location at which this equation is satisfied is the location of the vortex center plane MM'.

The location of the reattachment point for two-dimensional step flow and for axisymmetric flow over bluff bodies has been determined by Abramovich[13] by a potential flow analysis. In the two-dimensional analysis, Abramovich assumes that a mass of fluid moving through the circulation zone in the same direction as the unperturbed stream passes through the segment 3A (Fig. 12). A plane AF is drawn through A parallel to the plane of symmetry at a distance h from it, and terminates at a section Oy, which is a distance x_n from A. A new orthogonal coordinate system is defined such that the x-axis lies along the axis of symmetry and y axis passes through the point F. The results of Abramovich's analysis how that, over a wide R/h_n range,

$$h_n = 0.46B \qquad (28)$$

For the present geometry under consideration R/B = 3.20, therefore $R/h_n = 6.96$, which is within the range $3 \leq \frac{R}{h_n} \leq 10$ analyzed by Abramovich.

Equation (28) shows that the cross-sectional area of the back flow at the point x=0 is 46% of the total cross section of the circulation zone at the plane KK′. Assuming that this same area relationship holds for the axisymmetric case, the axisymmetric form of Eq. (28) is

$$R^2-(R-h_r)^2 = 0.46\left[R^2-(R-B)^2\right] \tag{29}$$

where h_r is the axisymmetric equivalent of h_n. Thus,

$$h_r = R - \sqrt{R^2-0.46(2RB-B^2)} \tag{30}$$

For the plane flow case, Abramovich shows that the ordinate of the separating streamline at x=0 is

$$y_{3_n} = 1.75h_n \tag{31}$$

Satisfying the same ratio of cross sections for the axisymmetric case gives

$$R^2-(R-y_3)^2 = 1.75\left[R^2-(R-h_r)^2\right] \tag{32}$$

or

$$y_3 = R - \sqrt{R^2-1.75(2Rh_r-h_r^2)} \tag{33}$$

Eliminating h_r in Eq. (33) by use of Eq. (30) gives

$$y_3 = R - \sqrt{R^2-0.805(2RB-B^2)} \tag{34}$$

Denoting the reattachment point N as $x = x_R$ in the new coordinate system, the total area of the zero velocity surface

$$A_o = \int_0^{x_R} 2\pi(R-y_4)dx \tag{35}$$

But the equation for the zero velocity line is[10]

$$\frac{x_4}{x_R} = 1 - \left(\frac{y_4}{h_r}\right)^3 \tag{36}$$

Substituting for y_4 from Eq. (36) into Eq. (35) and integrating yields

$$A_o = 2\pi x_R\left(R - \tfrac{3}{4} h_r\right) \tag{37}$$

The ratio of A_o to the cross-sectional area of the back stream at x=0 is

$$\frac{A_o}{\pi\left[R^2-(R-h_r)^2\right]} = \frac{2x_R\left(R - \frac{3}{4} h_r\right)}{(2Rh_r-h_r^2)} \tag{38}$$

For the plane flow problem[13]

$$\frac{A_o}{h_n} = \left(\frac{x_R}{h}\right)_n \tag{39}$$

Assuming that the ratio of corresponding flow sections is the same for the axisymmetric and plane flow cases, Eqs. (38) and (39) give

$$\frac{2x_R\left(R - \frac{3}{4} h_r\right)}{(2Rh_r - h_r^2)} = \left(\frac{x_R}{h}\right)_n = 0.46\left(\frac{x_R}{B}\right)_n \tag{40}$$

The following equation was developed by Abramovich for the ratio of attachment distance to step height for the two-dimensional case

$$\frac{x_R}{B} = -1.6 \frac{R}{B} \log\left(1 - 0.92 \frac{B}{R}\right) \tag{41}$$

Equations (30), (40), and (41) give

$$x_R = \frac{-0.368(2R-B)R\log(1-0.92B/R)}{\left[R-0.75\left(R-\sqrt{R^2-0.46(2RB-B^2)}\right)\right]} \tag{42}$$

The distance x_n given in Ref. 10 is assumed to be the same in the axisymmetric case, i.e.,

$$x_n = -0.73\left[0.92 + \frac{R}{B}\log\left(1-0.46\frac{B}{R}\right)\right] B \tag{43}$$

The length ℓ_2 (Fig. 11) is given by

$$\ell_2 = x_R - x_n \tag{44}$$

A computer program was written for the solution of the equations presented in this analysis.

Abbott[14] presents a theoretical and experimental analysis for the case of two-dimensional turbulent step flow. Figure 13, which was taken from Ref. 14, shows the non-dimensional reattachment distance as a function of the step and channel heights. It is seen that his theoretical results do not match the experimental data for step heights greater than 1/5th of the initial channel height. He suggests that the two-dimensional free jet boundary defined by Tollmien may be used as an asymptate to extrapolate the analysis to large step/channel height ratios.

In applying the integral approach to two-dimensional step flows, Abramovich[13] suggests that the boundary layer thickness should be expressed as b = 0.3x. This value was used to compute the non-dimensional reattachment distance for two-dimensional steps, and the results of the analysis are compared with Abbot's experimental data in Fig. 13. It is seen that the theory accurately predicts the reattachment distance over the entire range of the experimental data.

In order for the integral theory to predict the reattachment distances for both the two-dimensional and axisymmetric step flows, it was necessary to assume that annular jet spreading rate is 27% less than that of the two-dimensional jet. This change in jet spreading rate is confirmed by the results of Launder[15], who found that his "standard" turbulence model predicts the rate of spread of a round jet 30% too high.

V.2 Differential Approach

The integral approach discussed in the last section is of value where quick estimates of global type parameters are of interest, e.g., reattachment length, and/or separation streamline. However, where more detailed information is of interest, such as detailed velocity or shear stress profiles, a more complete mathematical form governing equations must be solved. The successful prediction of steady, axisymmetric, turbulent, and recirculating flows requires a knowledge of the physical laws governing the transport, creation, and destruction of turbulence. This knowledge must be cast in mathematical form and a scheme for solving the resultant differential equations must be written into a computer program.

Recirculating flows are characterized by the following properties: 1) There is no single predominant direction of motion, e.g., backflow can be and is usually present in the chosen coordinates, 2) Turbulent diffusive transport is important in all coordinate directions. Recirculating flows are thus governed by the elliptic differential Navier-Stokes equations. No practical numerical treatment can span all the time and length scales of turbulence, and the time averaged equations, containing unknown convective correlations, must be solved. A solution of these nonlinear equations is only possible where a turbulence model can be formulated which prescribes how these correlations are to be found. The accuracy with which turbulence parameters can be predicted is largely dependent upon the accuracy of these models. In other words, the equations do not give the entire story and models based on simple physical concepts and experiment must be developed to bridge the gap between the equations and the actual flows.

In turbulent flows and, in particular, recirculating flows, the local turbulence structure depends strongly on events elsewhere in the flow. The turbulence model must account for this "transported" nature of turbulence. In recent years attempts

have been made to account for this "transported" nature by computing the development of the local turbulent kinetic energy and dissipation per unit mass as the flow develops and relating the local unknown correlation (Reynolds stress) to these quantities. The steady state time-smoothed equations, including the (two-equation) energy-dissipation effective-viscosity model for determining the turbulent fluxes, can be written in the following form:[15]

Continuity

$$\frac{\partial}{\partial x_i}(\rho U_i) = 0 \tag{45}$$

Momentum

$$\frac{\partial}{\partial x_j}(\rho U_i U_j) - \frac{\partial}{\partial x_j}\left(\mu \frac{\partial U_i}{\partial x_j} - \overline{\rho u_i u_j}\right) + \frac{\partial P}{\partial x_i} = 0 \tag{46}$$

Turbulence Energy

$$\frac{\partial}{\partial x_j}(\rho k U_j) - \frac{\partial}{\partial x_j}\left(\frac{\mu_{eff}}{\sigma_k}\frac{\partial k}{\partial x_j}\right) - \mu_t G + \rho\varepsilon = 0 \tag{47}$$

Turbulence Dissipation

$$\frac{\partial}{\partial x_j}(\rho \varepsilon U_j) - \frac{\partial}{\partial x_j}\left(\frac{\mu_{eff}}{\sigma_\varepsilon}\frac{\partial \varepsilon}{\partial x_j}\right) - \frac{C_1 \varepsilon}{k}\mu_t G + C_2 \frac{\varepsilon^2}{k} = 0 \tag{48}$$

Auxiliary

$$-\overline{\rho u_i u_j} \equiv \mu_t \left(\frac{\partial U_i}{\partial x_j} + \frac{\partial U_j}{\partial x_i}\right) \tag{49}$$

$$\mu_t = C_\mu \frac{\rho k^2}{\varepsilon} = \mu_{eff} - \mu \tag{50}$$

$$G \equiv \left(\frac{\partial U_i}{\partial x_j} + \frac{\partial U_j}{\partial x_i}\right)\frac{\partial U_i}{\partial x_j} \tag{51}$$

These equations in two dimensions have been written in finite-difference form using the method described by Spalding[16] and Runchal[17] and solved using a modified version of the SIMPLE[18, 19] computer program. Details concerning the solution procedure are given in the cited references and will not be discussed further. The turbulence model given by Equations 47, 48, and 50 contain five empirical coefficients. The following table gives the values of these coefficients recommended by Launder[20] based on computations of free shear flows.

Table 1

Values of Constants in Turbulence Model

C_μ	C_1	C_2	σ_k	σ_ε
0.09	1.44	1.92	1.0	1.3

Computer optimization of these constants for the data obtained using this investigation showed that a value of 1.7 instead of 1.9 for C_2 resulted in better agreement between theory and experiment.

VI. COMPARISON OF THEORY AND EXPERIMENT

Results of the integral analysis to the configuration are presented in Fig. 14. The dividing streamline, locus of flow reversal, and location of reattachment point are shown. It is seen that the agreement between theoretical and experimental results are quite good considering the simplified nature of the integral analysis.

In order to get numerical solutions of the elliptical differential equation set, boundary conditions must be prescribed around the entire solution domain. These conditions were known or measured at all boundaries except at the jet entrance. At the jet inlet only, the centerline mean velocity was measured. By numerically integrating the velocity profiles measured downstream of the step, the total mass flow was determined. Knowing the centerline velocity, the total mass flow, and that the entrance tube length was sufficient to assure fully developed pipe flow, a power law profile was determined and used as the mean velocity boundary condition at the jet inlet. The turbulent energy and dissipation profiles were taken from Klebanoff's measurements as reported by Hinze[1] for the Reynolds number nearest that calculated for the jet inlet.

Results of the differential analysis are shown in Figs. 14, 15, and 16. The predicted locus of flow reversal downstream of the sudden expansion is compared with measured data in Fig. 14. It is apparent that the predicted recirculation zone is initially thinner and the reattachment point further downstream than is experimentally observed. By changing the turbulence production and dissipation rates (C_1 and C_2 in the turbulence model), the reattachment length could be easily varied; however, when these quantities were changed such that the reattachment point was exactly predicted, the recirculation zone thickness and centerline velocity decay were incorrectly predicted. Use of the modeling constants discussed previously is a compromise whereby all quantities of interest are predicted with similar accuracy.

Figure 15 is a comparison of the predicted and measured centerline velocity decay. The predicted decay rate compares very well with the measured rate being exactly correct in the initial region and slightly slower downstream of the recirculation zone. This slower decay rate leads to fully developed flow conditions being predicted further downstream than would be experimentally observed. The comparison of a predicted and measured velocity profile within the recirculation zone (x/D = 0.75) is shown in Fig. 16. This figure shows the predicted rate of spread of the round jet to be too high. The source of this problem is a limitation of the present turbulent model. The model does not account for the time lapse between extra turbulent energy being supplied and the effect being felt in the dissipating motions.

VII. BIBLIOGRAPHY

(1) Morgenthaler, J. H., Zelazny, S. W., and Herendeen, D. L., "Combustor Correlation Technique," Bell Report Number 9500-920208, September 1971.

(2) Morgenthaler, J. H., Zelazny, S. W., and Rudinger, G., "Progress Report - High Speed Turbulent Mixing and Combustion Application to Advanced Air Breathing Propulsion Engines," Bell Report Number 9500-920212, November 1971.

(3) Zelazny, S. W., "Eddy Viscosity in Quiescent and Coflowing Axisymmetric Jets," AIAA Journal, Vol. 9, November 1971, pp. 2292-2294.

(4) Baker, A. J., Moon, L. F., Morgenthaler, J. H., and Peschke, W. T., "Fluid Mechanics and Combustion Technology," Bell Report Number 9500-920246, January 1972.

(5) Morgenthaler, J. H. and Zelazny, S. W., "Predictions of Axisymmetric Free Turbulent Shear Flows Using a Generalized Eddy Viscosity Approach," Proceedings of the NASA Workshop on Free Turbulent Shear Flows, Conference Proceedings, Vol. I, NASA SP-321, July 1972.

(6) Zelazny, S. W., "Modeling of Turbulent Axisymmetric Coflowing Streams and Quiescent Jets: A Review and Extension," PhD Dissertation, State University of New York at Buffalo, September 1972.

(7) Morgenthaler, J. H., Zelazny, S. W., and Rudinger, G., "Progress Report - High Speed Turbulent Mixing and Combustion," Bell Report Number 9500-920258, December 1972.

(8) Rudinger, G., "Wave Propagation in Suspensions of Solid Particles in Gas Flow," Applied Mechanics Reviews, Vol. 26, March 1973, pp. 273-279.

(9) Zelazny, S. W., Morgenthaler, J. H., and Herendeen, D. L., "Shear Stress and Turbulence Intensity Models for Coflowing Axisymmetric Streams," AIAA Journal, Vol. 11, August 1973, pp. 1165-1173.

(10) Morgenthaler, J. H. and Rudinger, G., "Progress Report - High Speed Turbulent Mixing and Combustion," Bell Report Number 9500-920316, November 1973.

(11) Zelazny, S. W., "Study of Methods for Modeling Centerline Mass Fraction Decay in Turbulent Jets," AIAA Journal, Vol. 12, No. 2, February 1974, pp. 235-237.

(12) Rudinger, G., "Experimental Investigation of Gas Injection Through a Transverse Slot into a Subsonic Cross Flow," AIAA Journal, Vol. 12, April 1974, pp. 566-568.

(13) Morgenthaler, J. H., "Turbulent Mixing and Reacting Flow Characterization," Fluid Mechanics of Combustion, ASME, New York, May 1974, pp. 21-34.

(14) Rudinger, G., "Effects of Velocity Slip on the Burning Rate of Fuel Particles," Fluid Mechanics of Combustion, ASME, New York May 1974, pp. 35-46.

(15) Rudinger, G., "Simultaneous Heat, Mass, and Momentum Addition to a Gas Flow in a Pipe," ASME Paper No. 74-FE-14, May 1974.

(16) Rudinger, G., "Penetration of Particles Injected into a Constant Cross Flow," AIAA Journal, Vol. 12, No. 8, August 1974, pp. 1138-1140.

(17) Morgenthaler, J. H., Moon, L. F., and Stepien, W. R., "Developing a Gas Rocket Performance Prediction Technique," NASA CR-134728, October 1974.

(18) Rudinger, G., "Progress Report - High Speed Turbulent Mixing and Combustion," Bell Report Number 9500-920351, November 1974.

(19) Moon, L. F. and Zelazny, S. W., "Experimental and Analytical Study of Jet Noise Modeling," AIAA Journal, Vol. 13, No. 3, March 1975, pp. 387-393.

(20) Rudinger, G., "Effect of Velocity Slip on the Burning Rate of Fuel Particles," Journal of Fluids Engineering, Trans. ASME, Vol. 97I, No. 3, September 1975, pp. 321-326.

(21) Moon, L. F., Rudinger, G., and Salter, G. R., "Final Report - High Speed Turbulent Mixing and Combustion," Bell Report Number 9500-920350, November 1975.

(22) Morgenthaler, J. H., "Turbulent Mixing and Reacting Flow Characterization," scheduled for publication in the Journal of Fluids Engineering, Trans. ASME, December 1975.

(23) Rudinger, G., "Fundamentals and Applications of Gas-Particle Flow," to be published in a forthcoming AGARDograph.

(24) Rudinger, G., "Some Aspects of Gas-Particle Jets in a Cross Flow," submitted for publication in the ASME Journal.

(25) Moon, L. F., Rudinger, G., and Salter, G. R., "Velocity Distribution in an Abruptly Expanding Circular Duct," submitted for publication in the ASME Journal.

REFERENCES

1. Hinze, J. O., Turbulence, McGraw-Hill, 1959.

2. Launder, B. E. and Spalding, D. B., Mathematical Models of Turbulence, Academic Press, 1972.

3. Swithenbank, J., "Some Unresolved Problems in the Fluid Mechanics of Combustion," Journal of Fluid Engineering, Transactions ASME, Vol. 97I, September 1975, pp. 287-296.

4. Chigier, N. A., "Gas Dynamics of Swirling Flow in Combustion Systems," Astronautica Acta, Vol. 17, 1972, pp. 387-395.

5. United Aircraft Corporation Research Laboratory, "Demonstration of HF Chain Reaction Laser," Technical Report RK-CR-75-4, July 1974.

6. Liu, Y. H., Whitby, K. T., and Yu, H. H. S., "A Condensation Aerosol Generator for Producing Monodispersed Aerosols in the Size Range 0.036 μm to 1.3 μm," Journal de Recherches Atmospheriques, Vol. 2, 1966, pp. 397-406.

7. Stevenson, W. H. and Thompson, H. D., Editors, "The Use of the Laser-Doppler Velocimeter for Flow Measurements," Project SQUID Workshop, Purdue University, March 1972.

8. Bradshaw, P., An Introduction of Turbulence and Its Measurement, Pergamon Press, 1971.

9. Back, L. H. and Roschke, E. J., "Shear-Layer Flow Regimes and Wave Instabilities and Reattachment Lengths Downstream of an Abrupt Circular Channel Expansion," Journal of Applied Mechanics, Transactions ASME, Vol. 94, September 1972, pp. 677-881.

10. Krall, K. M. and Sparrow, E. M., "Turbulent Heat Transfer in the Separated Reattached and Redevelopment Regions of a Circular Tube," Journal of Heat Transfer, Transactions ASME, Vol. 88, February 1966, pp. 131-136.

11. Runchal, A. K., "Mass Transfer Investigation in Turbulent Flow Downstream of Sudden Enlargement of a Circular Pipe for Very High Schmidt Numbers," International Journal of Heat and Mass Transfer, Vol. 14, 1971, pp. 781-791.

12. Schlichting, H., Boundary Layer Theory, 4th Edition, McGraw-Hill, 1960, Chapters XVIII to XX.

13. Abramovich, G. N., The Theory of Turbulent Jets, MIT Press, 1963.

14. Abbott, D. E., "Analytical Investigation of Subsonic Turbulent Flow Over Single Backward Facing Steps," Vidya, Inc., Palo Alto, California Report, 1961.

15. Launder, B. E., "Turbulence Models and Their Experimental Verification," Imperial College M.E.D. Report HTS/73/26, 1973.

16. Spalding, D. B., "A Novel Finite Difference Formulation for Differential Expressions Involving Both First and Second Derivatives," International Journal of Numerical Methods in Engineering, Vol. 4, 1972, pp. 551-559.

17. Runchal, A. K., "Convergence and Accuracy of Three Finite Difference Schemes for a Two-Dimensional Conduction and Convection Problem," International Journal of Numerical Methods in Engineering, Vol. 4, 1972, pp. 541-550.

18. Patankar, S. V. and Spalding, D. B., "A Calculation Procedure for Heat, Mass, and Momentum Transfer in Three-Dimensional Parabolic Flows," International Journal of Heat and Mass Transfer, Vol. 15, 1972, pp. 1787-1806.

19. Caretto, L. S., Gosman, A. D., Patankar, S. V., and Spalding, D. B., "Two Calculation Procedures for Steady Three-Dimensional Flows with Recirculation," Proceedings 3rd Industrial Conference on Numerical Methods in Fluid Mechanics, Springer Verlag, 1972.

20. Launder, B. E., Progress in the Modeling of Turbulent Transport, Pennsylvania State University, Supplementary Notes for Course "Turbulent Recirculating Flows-Prediction and Measurement," 1975.

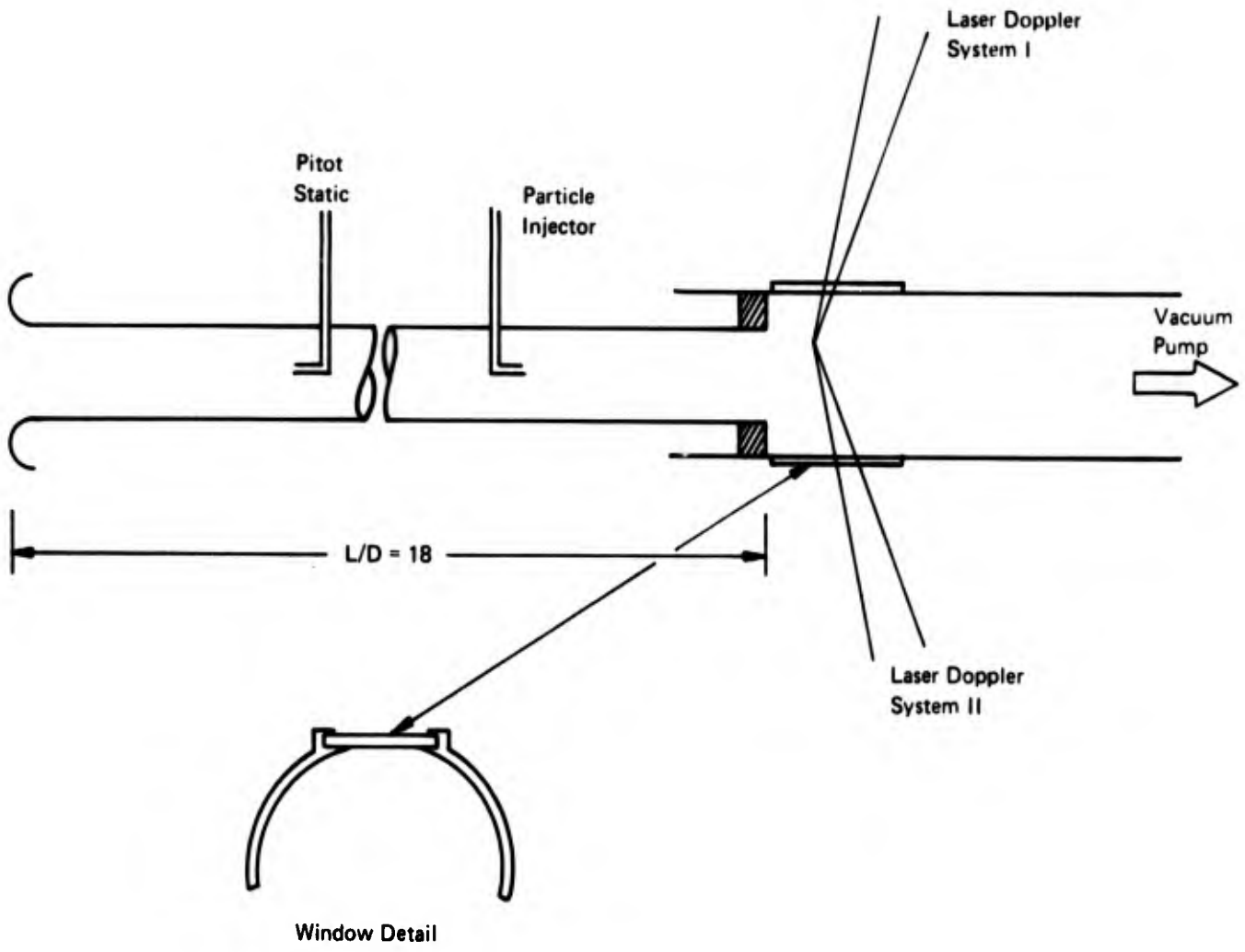

Figure 1. Schematic of Test Section

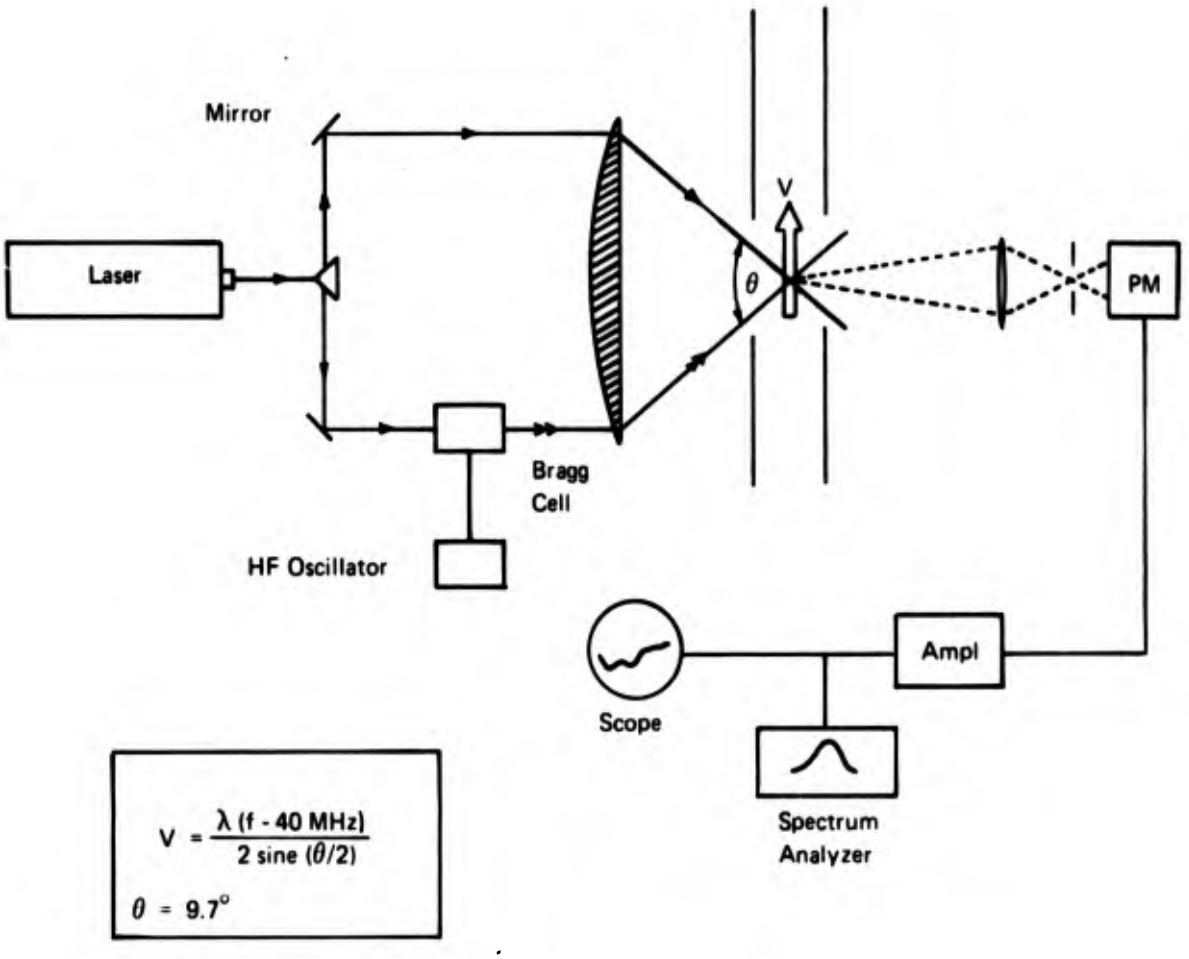

Figure 2. Schematic of Laser Doppler Velocimeter

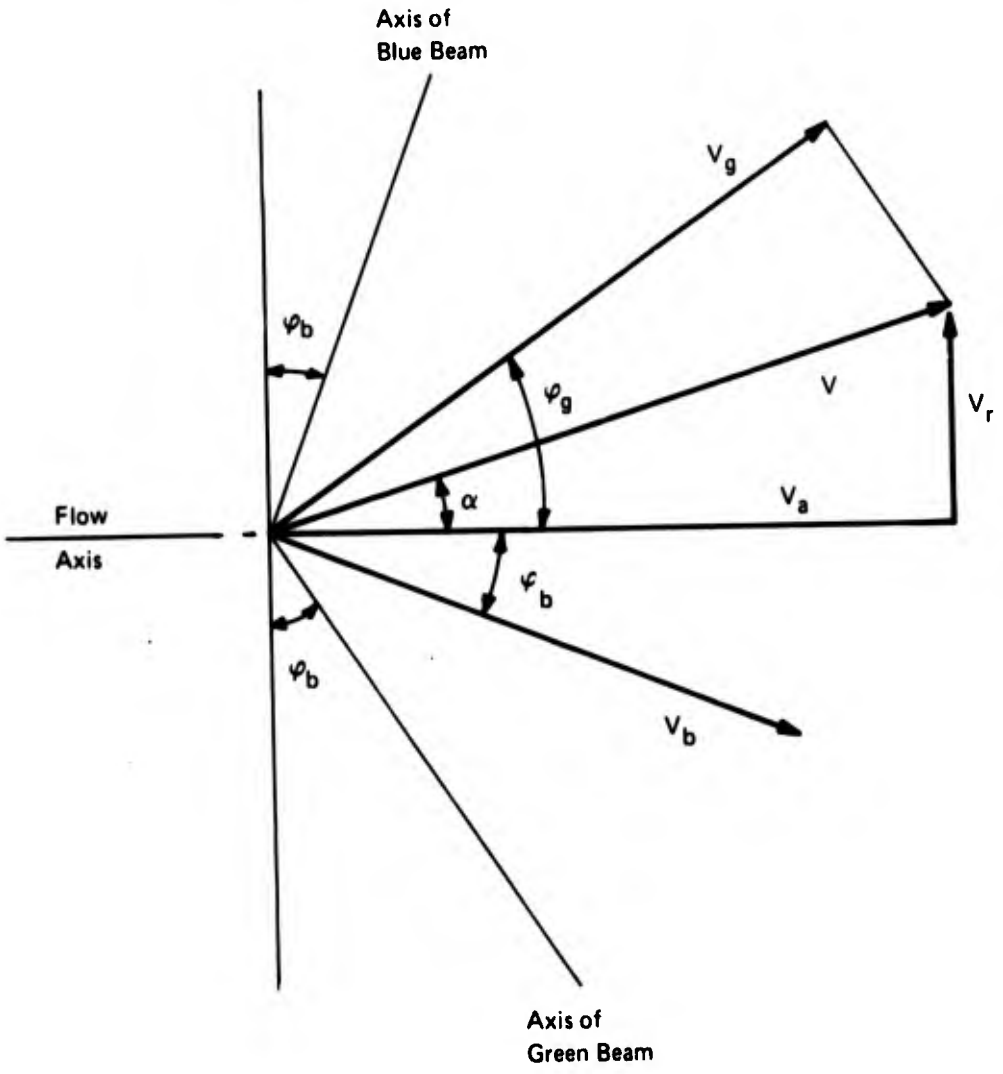

Figure 3. Coordinate System used for Velocity Measurements

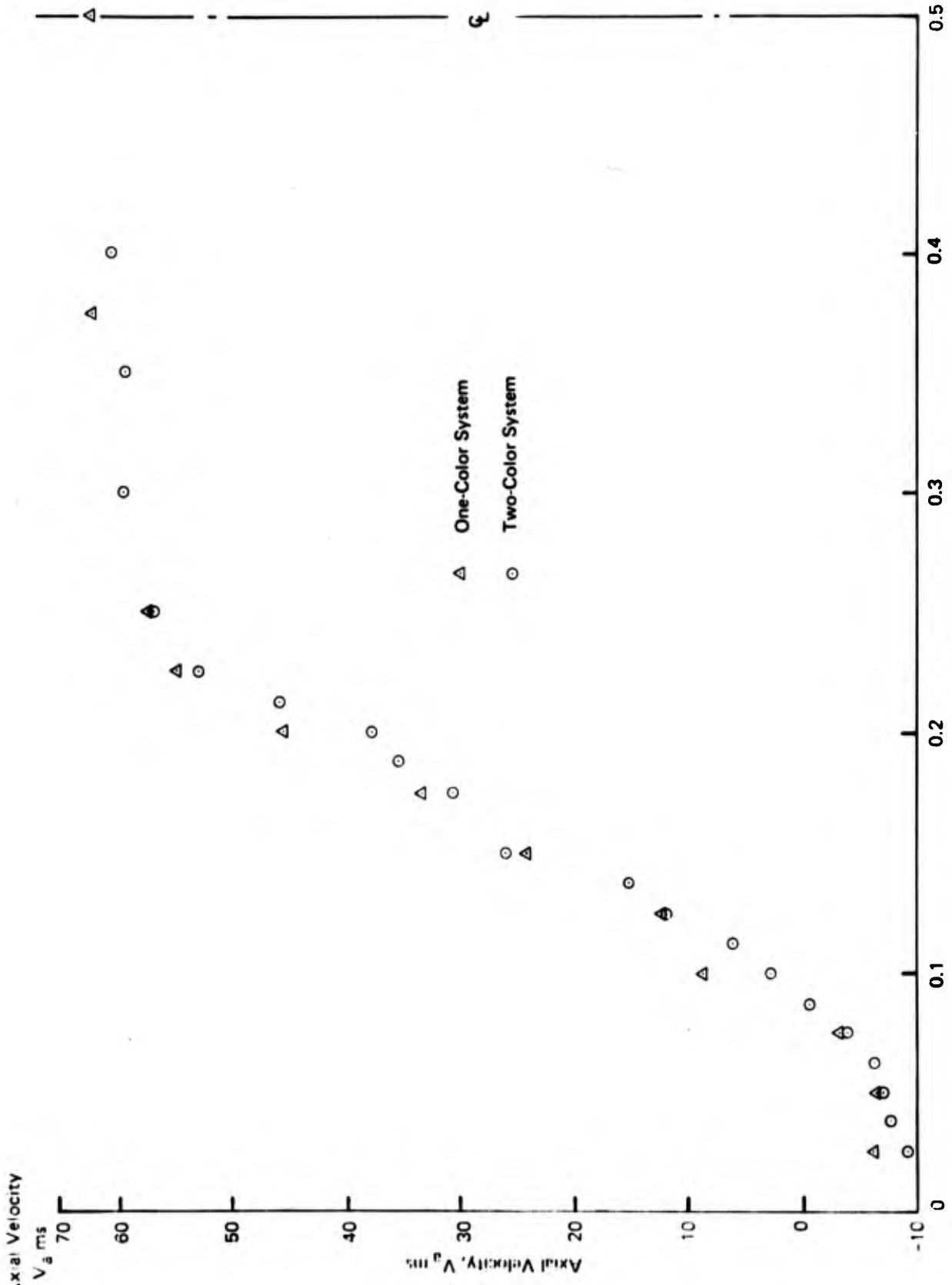

Figure 5. Velocity Profile at x/D = 0.75

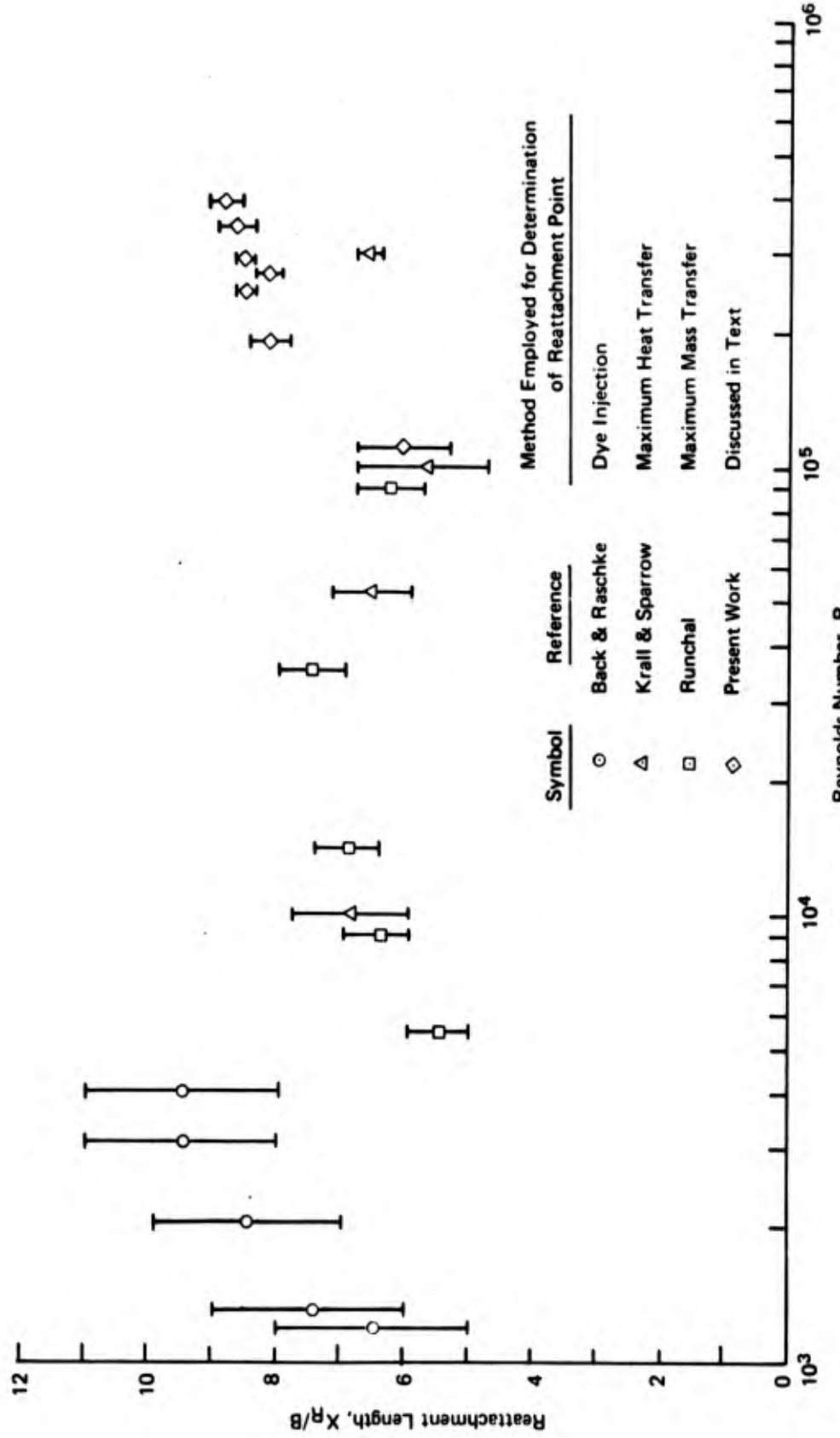

Figure 4. Variation of Reattachment Length with Reynolds Numbers

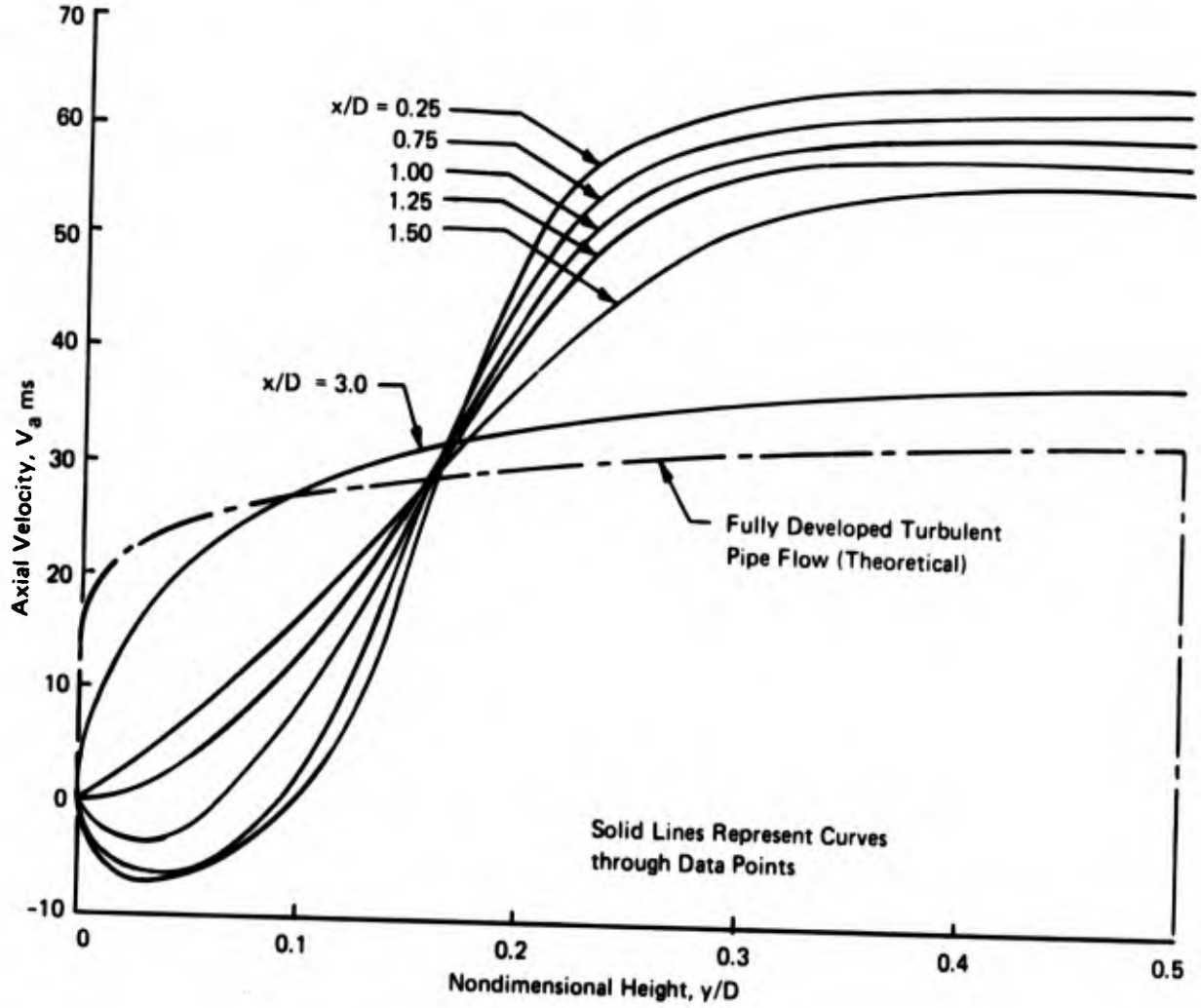

Figure 6. Velocity Profiles Measured at Six Locations Downstream of the Step

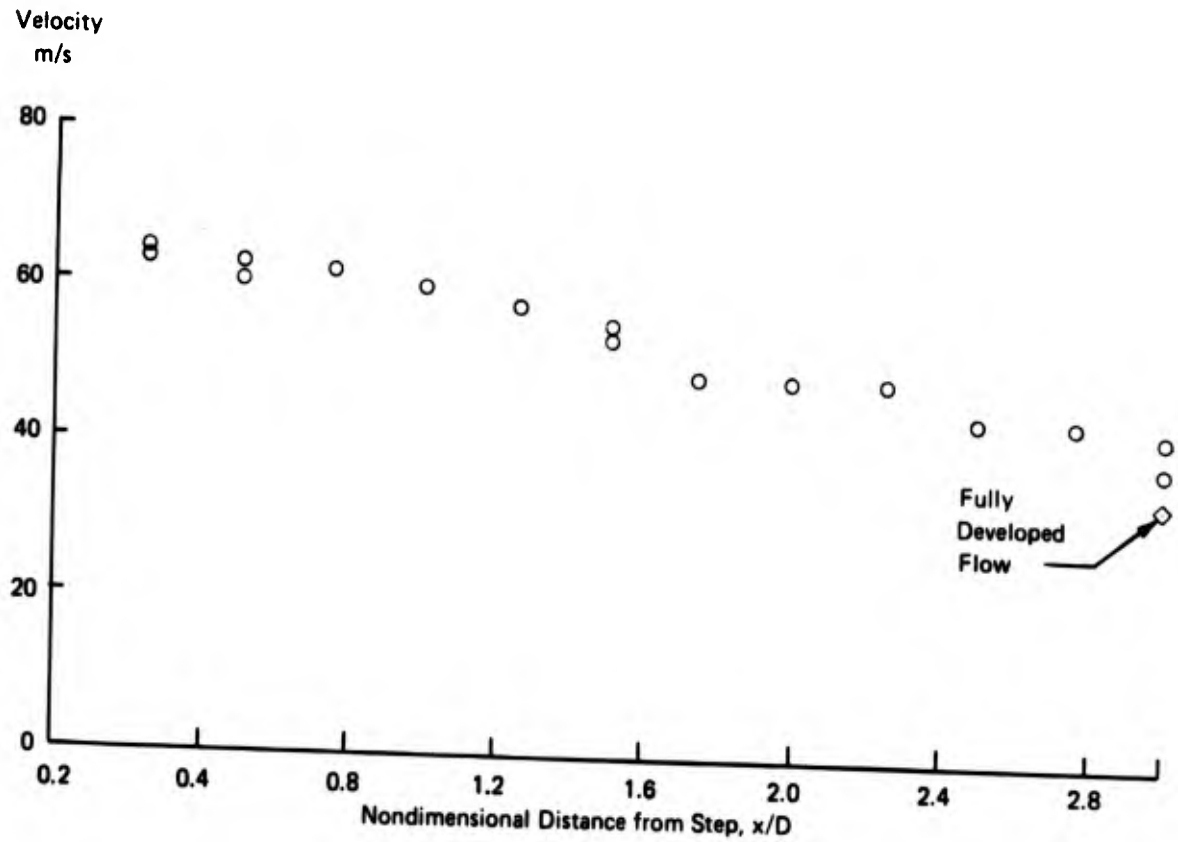

Figure 7. Axial Velocity on Centerline

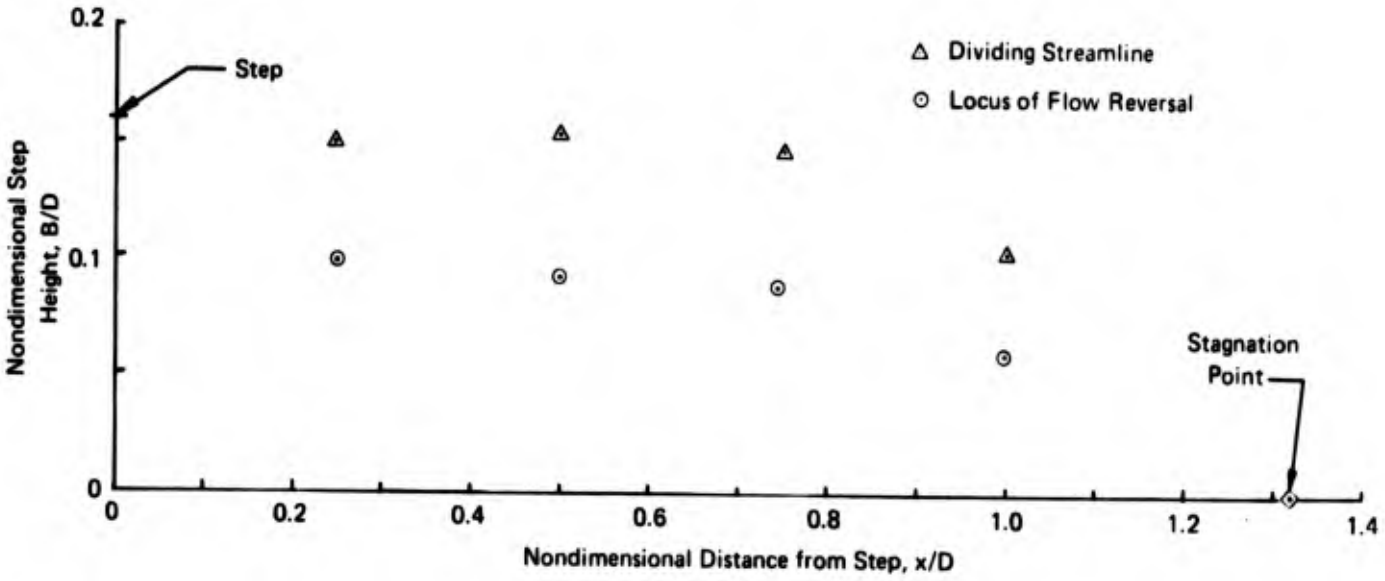

Figure 8. Experimently Determined Recirculation Zone

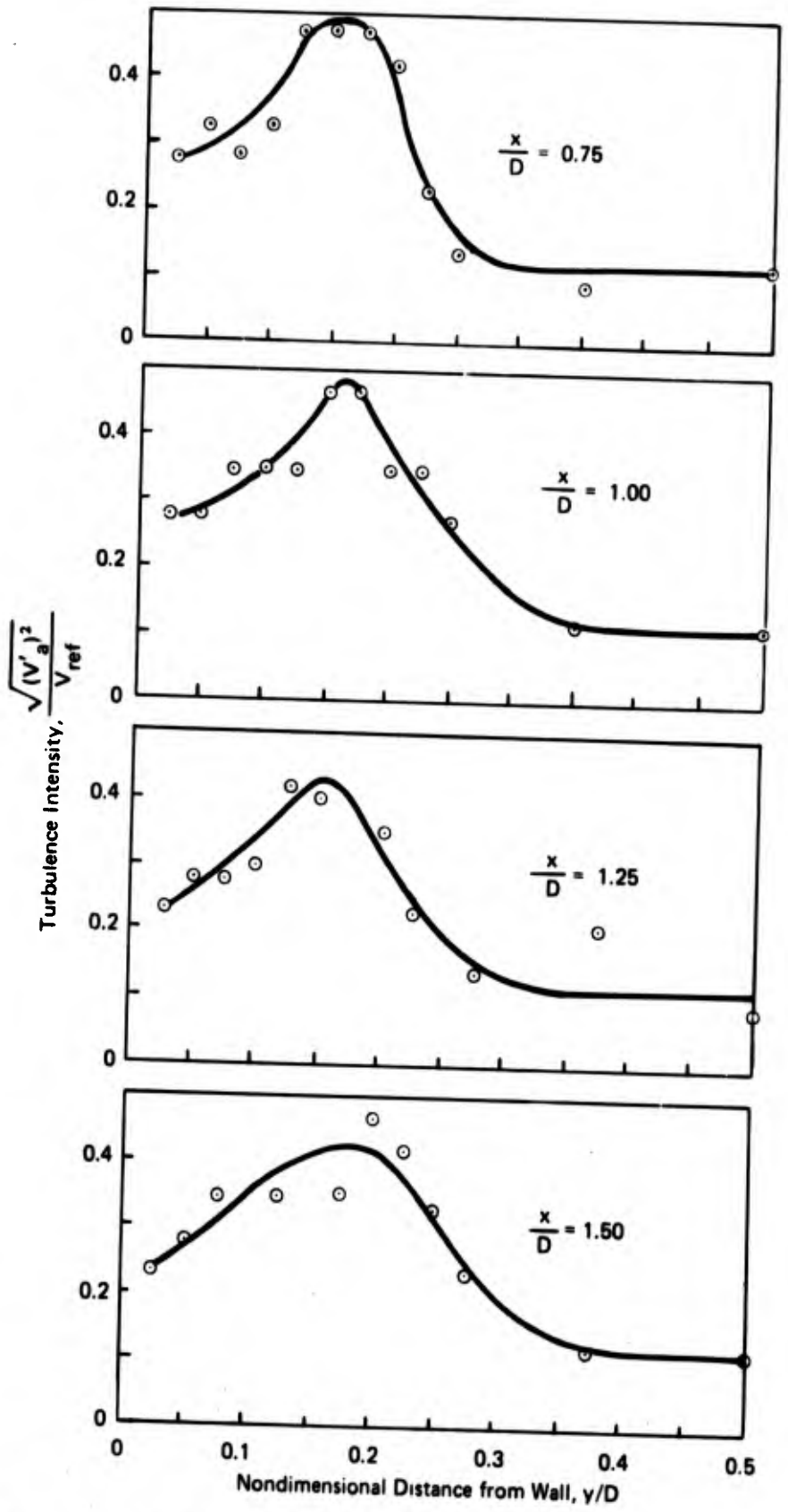

Figure 9. Axial Turbulence Intensity Profile (Lines are Curve Fits of Data)

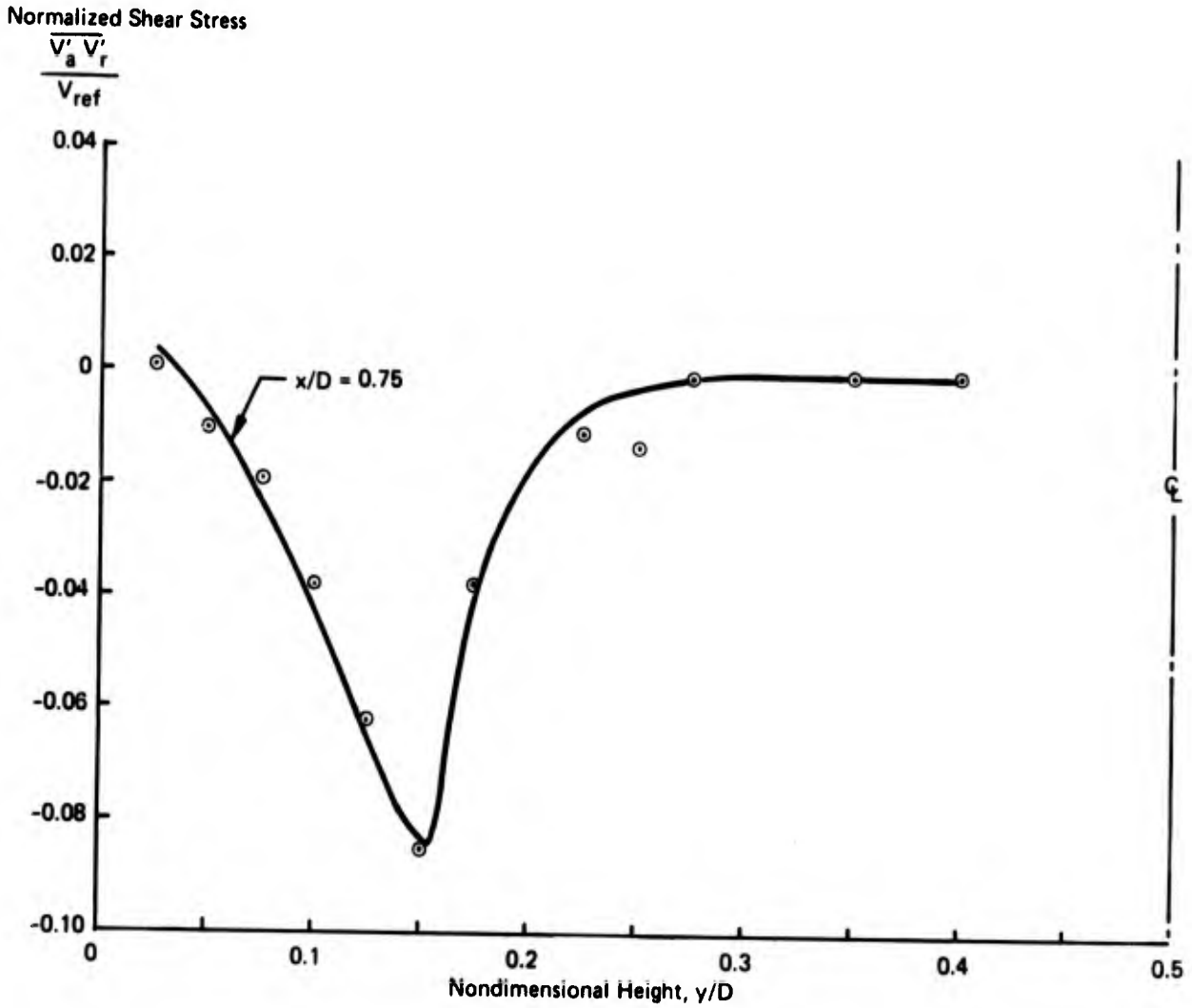

Figure 10. Normalized Shear Stress Profile (Line is Curve Fit of Data)

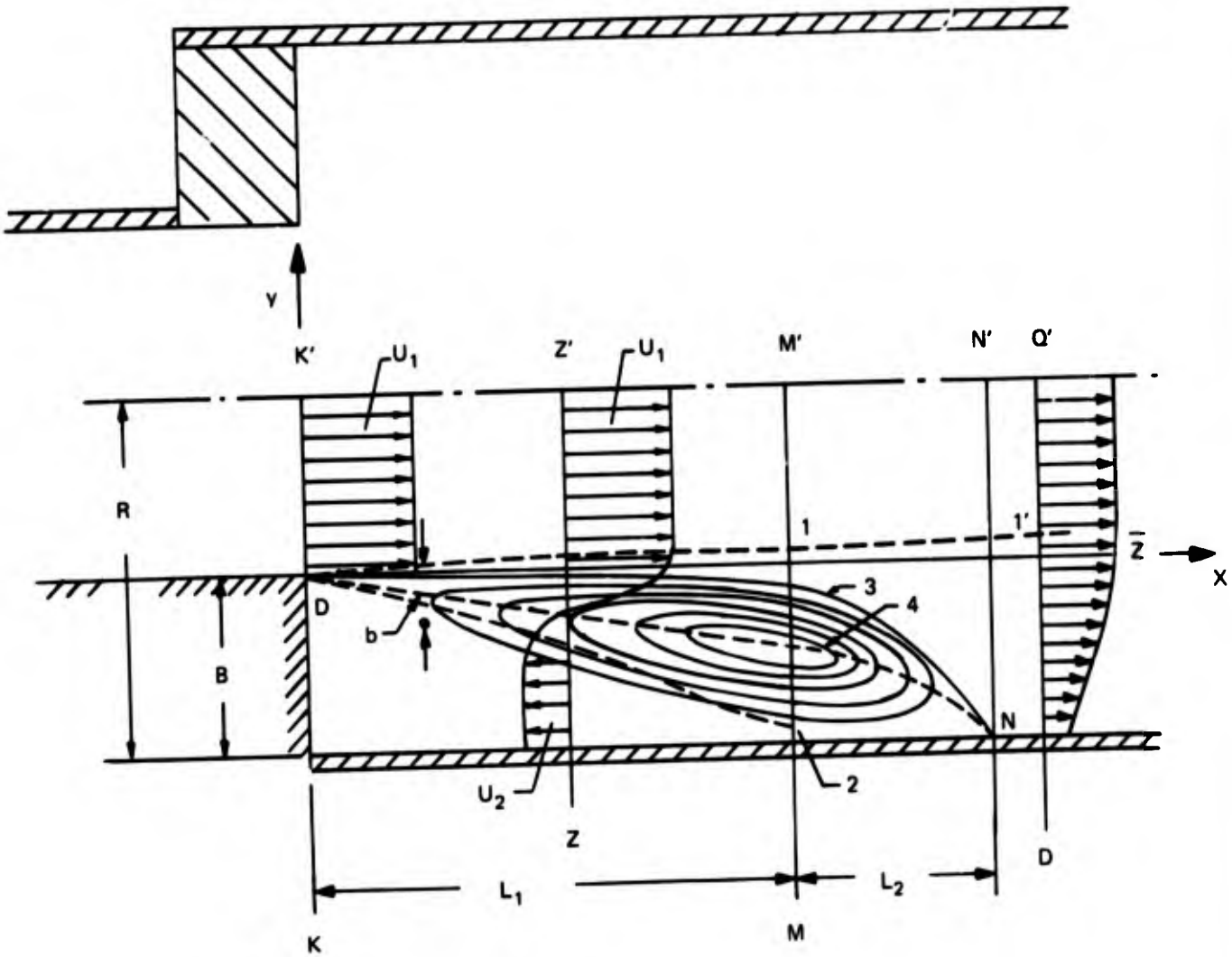

Figure 11. Theoretically Defined Recirculation Zone

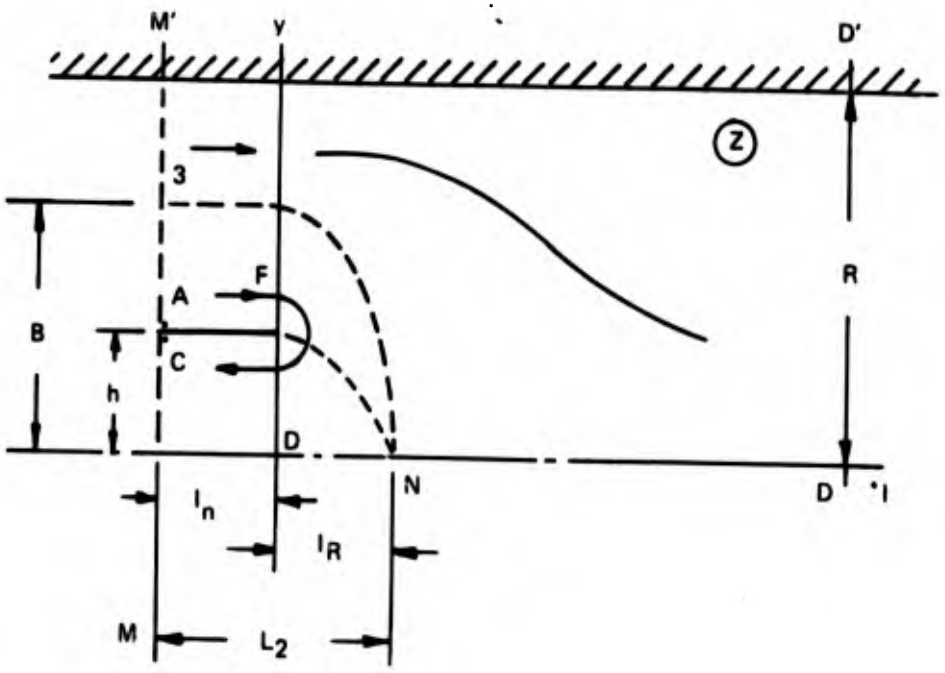

Figure 12. Coordinate System used in Integral Analysis

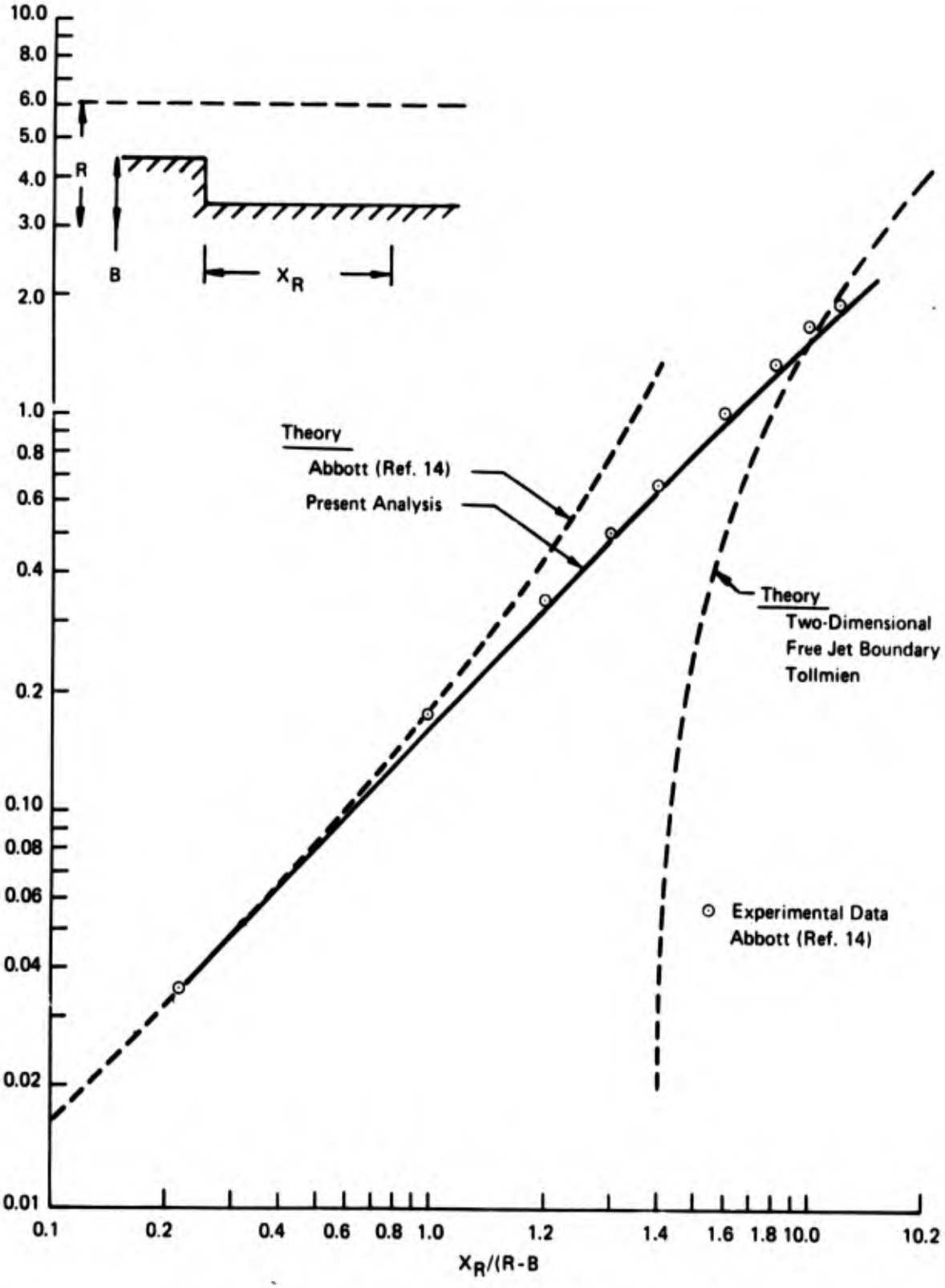

Figure 13. Two-Dimensional Step Reattachment Distance

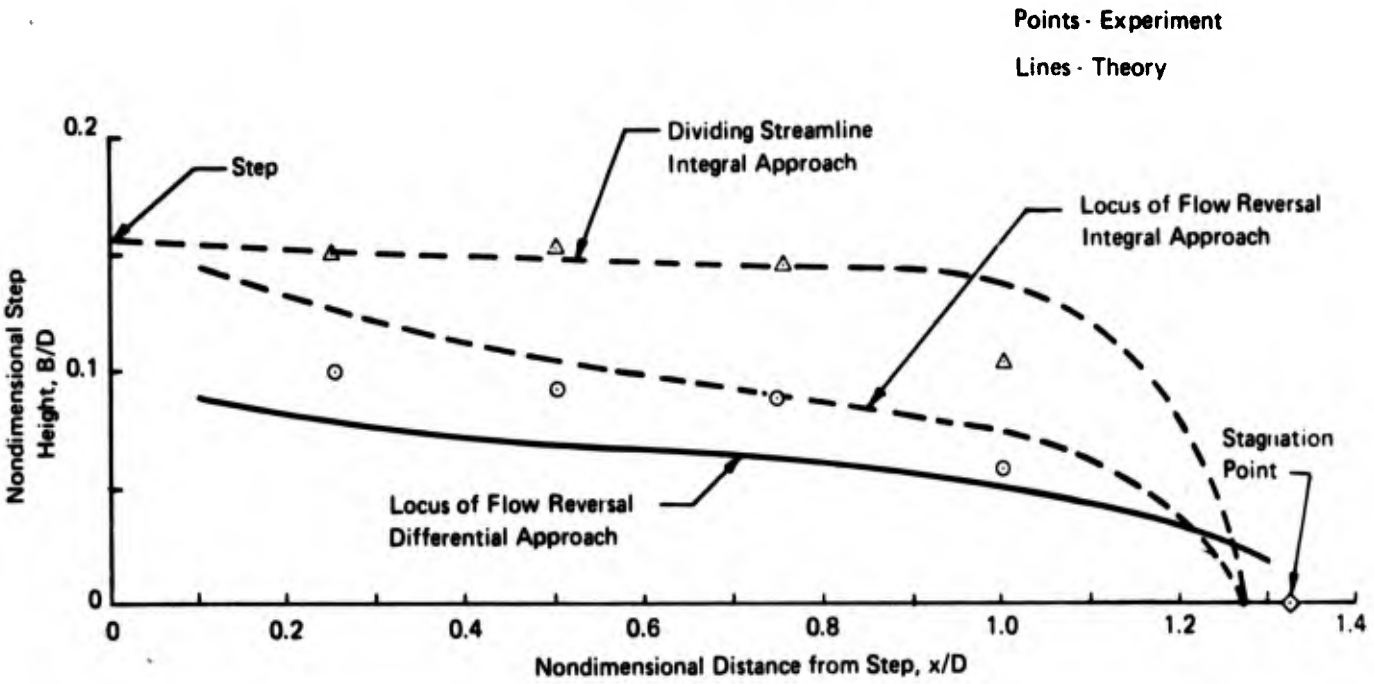

Figure 14. Recirculation Zone

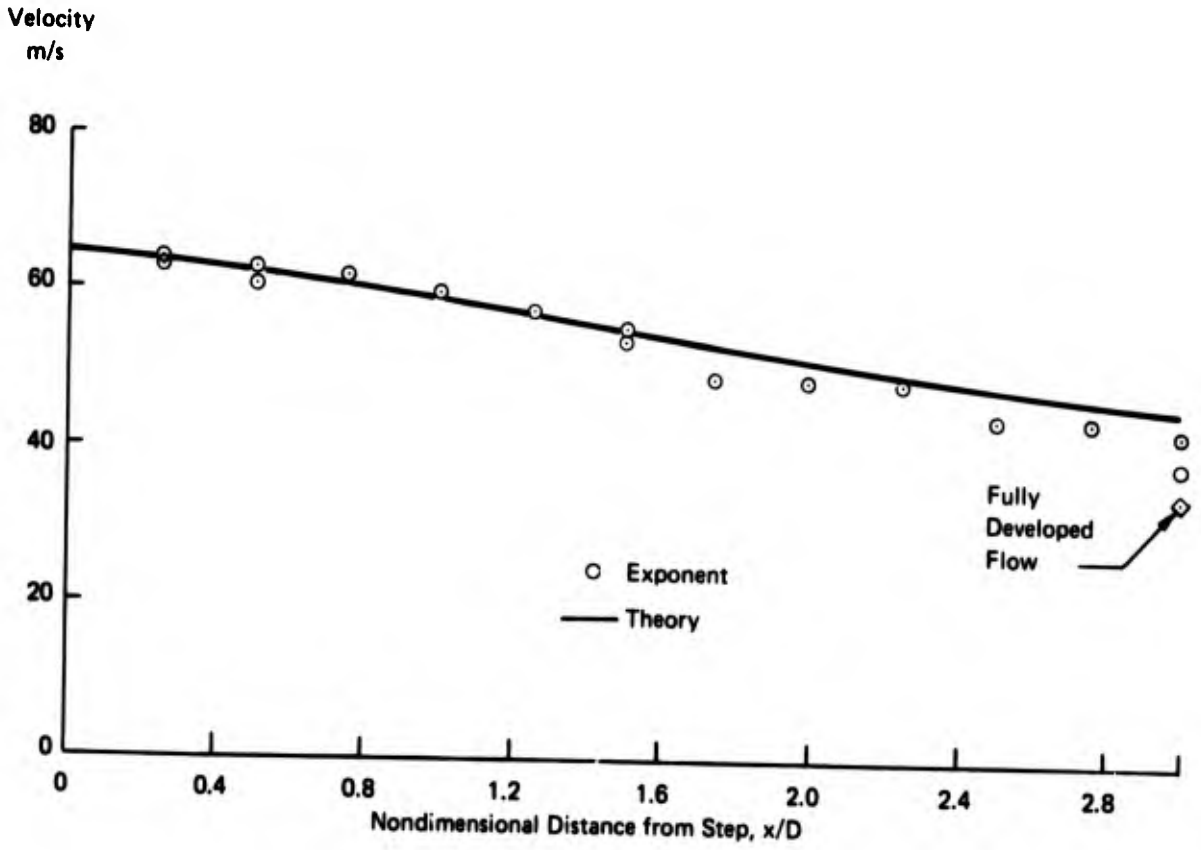

Figure 15. Comparison of Measured Centerline Velocity with Prediction

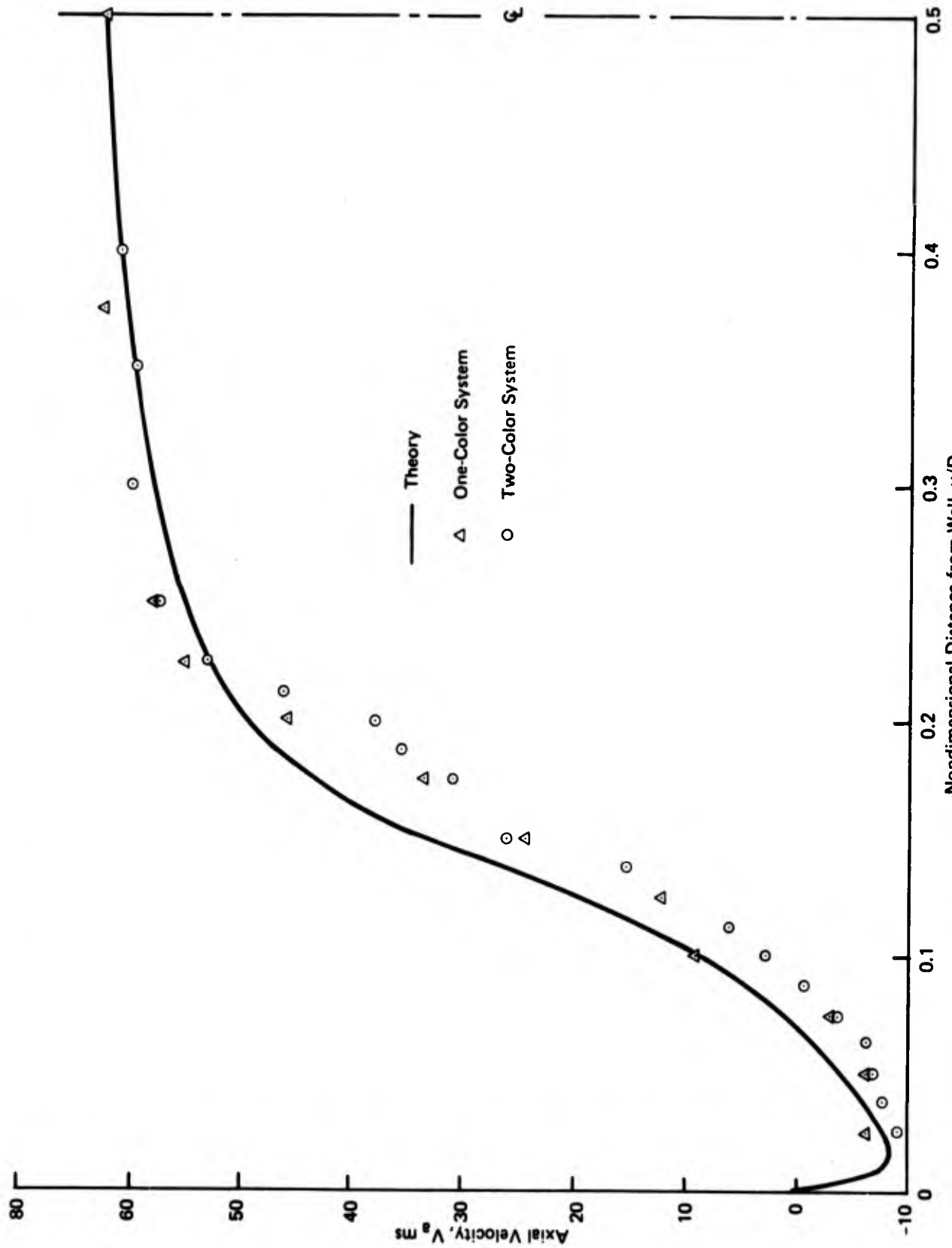

Figure 16. Comparison of Predicted and Measured Velocity Profile at X/D = 0.75

UNCLASSIFIED

SECURITY CLASSIFICATION OF THIS PAGE (When Data Entered)

REPORT DOCUMENTATION PAGE

READ INSTRUCTIONS BEFORE COMPLETING FORM

1. REPORT NUMBER: AFOSR-TR-75-1648

2. GOVT ACCESSION NO.

3. RECIPIENT'S CATALOG NUMBER

4. TITLE (and Subtitle): TURBULENT MIXING AND COMBUSTION.

5. TYPE OF REPORT & PERIOD COVERED: FINAL rept. Aug 70-Jul 75

6. PERFORMING ORG. REPORT NUMBER: 9500-920350

7. AUTHOR(s): L. F. MOON, G. RUDINGER, G. R. SALTER

8. CONTRACT OR GRANT NUMBER(s): F44620-70-C-0116

9. PERFORMING ORGANIZATION NAME AND ADDRESS
BELL AEROSPACE COMPANY
DIVISION OF TEXTRON
P O BOX ONE, BUFFALO, N Y 14240

10. PROGRAM ELEMENT, PROJECT, TASK AREA & WORK UNIT NUMBERS
681308
9711-02
61102F

11. CONTROLLING OFFICE NAME AND ADDRESS
AIR FORCE OFFICE OF SCIENTIFIC RESEARCH/NA
BUILDING 410
BOLLING AIR FORCE BASE, D C 20332

12. REPORT DATE: Nov 75

13. NUMBER OF PAGES: 57 (60p.)

14. MONITORING AGENCY NAME & ADDRESS (if different from Controlling Office): AF-6813, AF-9711

15. SECURITY CLASS. (of this report): UNCLASSIFIED

15a. DECLASSIFICATION/DOWNGRADING SCHEDULE

16. DISTRIBUTION STATEMENT (of this Report): 2

Approved for public release; distribution unlimited.

17. DISTRIBUTION STATEMENT (of the abstract entered in Block 20, if different from Report)

18. SUPPLEMENTARY NOTES

19. KEY WORDS (Continue on reverse side if necessary and identify by block number)
SUBSONIC TURBULENT MIXING
SUDDEN DUMP COMBUSTORS
AIR-BREATHING COMBUSTORS
CHEMICAL LASERS
RECIRCULATING FLOWS

20. ABSTRACT (Continue on reverse side if necessary and identify by block number)
The behavior of recirculating flows typical of advanced air-breathing and rocket injectors, as well as high energy chemical lasers, have been experimentally investigated. The configuration used consisted of a circular duct having a sudden increase of its diameter. Step size and flow velocity were chosen to be of a magnitude representative of "sudden-dump" combustion chambers. The recirculation, which occurred in the separation region behind the sudden expansion, was investigated using a laser-Doppler velocimeter. Detailed measurements of the mean, axial, and radial velocities were made, as well as some measurements of

DD FORM 1 JAN 73 1473 EDITION OF 1 NOV 65 IS OBSOLETE

UNCLASSIFIED

SECURITY CLASSIFICATION OF THIS PAGE (When Data Entered)

054000

turbulence intensity and shear stress. A set of partial differential equations - including continuity, axial and transverse momentum, turbulence energy, and turbulence dissipation - were derived and simultaneously solved using both intergral and finite differencing techniques. Predictions made using these equations were brought into good agreement with the data taken from the recirculating flows under investigation by computer optimization of appropriate "constants" in the models.